Distributed Symmetric Turbo Coded OFDM Scheme Incorporated with STBC-MIMO Antennas for Coded-Cooperative Wireless Communication under Wideband Noise Jamming Environment

Agha M. Ali MIRZA [1,2], Attaullah KHAWAJA [3], Shoaib MUGHAL [4], Rizwan A. BUTT [1]

[1] Dept. of Telecommunication Engineering, NED University of Engineering and Technology, Karachi, Pakistan
[2] Dept. of Electrical Engineering, Sir Syed University of Engineering and Technology, Karachi, Pakistan
[3] Dept. of Electrical Engineering, NED University of Engineering and Technology, Karachi, Pakistan
[4] Dept. of Computer Engineering, Bahria University Karachi Campus, Karachi, Pakistan

mamirza@ssuet.edu.pk, atta@neduet.edu.pk, shoaibmughal.bukc@bahria.edu.pk, rizwan.aslam@neduet.edu.pk

Submitted March 25, 2024 / Accepted July 1, 2024 / Online first August 19, 2024

Abstract. *This research paper proposes a novel anti-jamming technique based on a single-relay distributed symmetric Turbo coded orthogonal frequency division multiplexing (DSTC-OFDM) scheme. The stated scheme is incorporated with Alamouti space-time block code (STBC) multiple-input multiple-output (MIMO) 2×2 antennas for coded-cooperative wireless communication system under wideband noise jamming environment. As a suitable benchmark for comparison, a conventional symmetric Turbo coded OFDM (STC-OFDM) scheme incorporated with Alamouti STBC-MIMO (2×2) antennas is also developed for non-cooperative wireless communication system under the same jamming environment. Moreover, both the proposed MIMO schemes are compared with the corresponding single-antenna schemes. In this research, the modulation techniques employed are binary phase-shift keying and M-ary quadrature amplitude modulation while soft-demodulators are used at the destination node along with a joint iterative soft-input/soft-output decoding technique. According to the Monte Carlo simulation results, the proposed DSTC-OFDM-MIMO (coded-cooperative) scheme with Alamouti-STBC (2×2) antennas outperforms the STC-OFDM-MIMO (non-cooperative) scheme by a gain that ranges between 0.5–6 dB for different jamming scenarios in the high SNR simulated region under the same conditions, i.e., the code rates $R_c = 1/3$ and data frame lengths $l = 512$ bits for both the proposed schemes. However, in the low SNR simulated region, the STC-OFDM-MIMO scheme shows similar performance as the DSTC-OFDM-MIMO scheme, under identical conditions. Furthermore, the proposed distributed scheme with STBC-MIMO (2×2) antennas incorporates both coding gain and cooperative diversity gain.*

Keywords

Alamouti space-time block coding, anti-jamming technique, distributed symmetric Turbo code, multiple-input multiple-output, orthogonal frequency division multiplexing, wideband noise jamming

1. Introduction

In wireless communication, one of the most widely employed methods to limit the effectiveness of an adversary's communication is known as jamming in which the signal of an authorized user is deliberately interfered with or blocked by the opponent [1]. Due to the evolution of on-ground vehicular ad-hoc networks (VANETs) and in-air unmanned aerial vehicular (UAV) networks, secure wireless communication links have become an essential requirement [2]. The demand for jammer-aware or jammer-resilient systems, which are capable of sustaining communication links under noisy and jamming environments, is rising as the requirement for safety-critical vehicular and tactical communications increases [3], [4]. Previously, jamming attacks were limited only to battlefields and military operations. However, with the widespread use of different wireless devices, such as mobile phones, tablets, PDAs etc., and particularly with the advent of user-configurable intelligent devices, jamming attacks have now posed a serious and urgent threat to both civilian and commercial communications [5].

Apart from voice networks, the concept of jamming radio frequency (RF) signals can also be utilized in wireless data networks to corrupt information as well as disrupt its flow. As a result, the desired wireless signal cannot be received or decoded properly at the receiving end of the wireless communication network [6]. Thus, RF jamming has significantly drawn the attention of researchers as a major issue and several studies have already addressed different aspects of RF jamming techniques as well as the counter strategies for the last couple of decades [1]. RF jammers work by transmitting radio signals through which communication is disrupted by decreasing the signal-to-

DOI: 10.13164/re.2024.0502

noise ratio (SNR). It impairs communication to a significant level and exposes wireless communication systems to security vulnerabilities.

Various types of jamming attacks on wireless communication networks and anti-jamming (AJ) strategies to counter those attacks have been covered in the literature [1], [3]. There are several different types of jamming attacks which can be employed for jamming communications systems; however, the most appropriate choice depends on the type of communication system being targeted and the jamming strategy employed [7]. The specific type of jamming attack considered in this research study is wideband noise jamming also known as barrage jamming attack in which the adversary constantly emits noise energy across the whole frequency-spectrum of communication channels. These barrage jamming attacks fall under the category of non-protocol aware jamming since the adversary can carry out the attacks without any prior knowledge of the communication protocol [8]. A broadband jammer can degrade the effective bandwidth (BW) of a jammed communication link, by directly injecting wideband noise interference into the entire communication system, thereby reducing the achievable SNR of the signal [3]. In this case, the jammer emits the wideband Gaussian noise which is uniformly spread over the entire frequency-range of the signal, thereby lowering the resultant SNR of the receiver [6]. As a result, it degrades the bit error performance and reduces the effective BW of the jammed communication link.

Although in the past decades, wireless communication technologies have made significant advances, most wireless networks are still vulnerable to noise jamming attacks. Due to the exposed nature of wireless channels, the progress in designing jamming-resilient wireless communication systems still remains inadequate. However, in the existing literature [2], several AJ strategies have already been proposed and developed to exclude or counter the effects of jamming attacks, which can be categorized into the following classes: channel coding protection, channel hopping, spectrum spreading, multiple-input multiple-output (MIMO) based jamming mitigation, jamming detection mechanisms, rate adaptation and power control techniques. Provided the harmfulness of jamming threats and the complexity of wireless communication networks, no single common or non-specific solution can counter all sorts of jamming attacks. In particular, the core limitation of the current AJ techniques is that none of them can alone fully combat the potential effect of wideband noise or barrage jamming attacks. In practice, a combination of different AJ techniques, including frequency hopping, spread spectrum and forward error correction (FEC) codes may be employed to enhance the overall AJ capabilities of a communication system. Perhaps the most popular and widely used of these AJ techniques is to employ FEC Channel coding techniques. Various FEC channel codes have already been proposed, such as Reed-Solomon (RS) codes [9], Extended Bose-Chaudhuri-Hocquenghem (eBCH) codes [10], Low-Density Parity-Check (LDPC) codes [11], [12], and Turbo codes [13], [14], as a way to reduce the potential effect of jamming environment.

Recent research advances in wireless communication have shown that a Turbo coded system (TCS) is one of the most suitable and effective AJ techniques which significantly reduces the bit error rate (BER) [13], [14], [15]. Turbo codes, a class of FEC codes, were originally developed for use in communication systems to provide robust error correction in the presence of noise and interference [16]. While their primary purpose is not specifically designed for AJ, their inherent error-correcting capabilities can contribute to robust communication in the presence of deliberate interference or noise jamming. Although not particularly designed as an AJ technique, Turbo codes are well-known for their superior performance in noisy channels and their ability to combat noise can be beneficial in scenarios where jamming introduces additional noise. Although Turbo codes can enhance the resilience of communication systems against interference, the effectiveness of AJ measures may also depend on the specific characteristics of the jamming signals and the overall system design. However, the performance of TCS depends on different parameters, namely code rate, frame length, component recursive systematic convolutional (RSC) codes, interleaver design, decoding iterations, and distance spectrum [17], [18].

In mitigating the effects of wideband noise jamming attacks, diversity techniques can also play a crucial role. A relatively new diversity scheme, generally referred to as user-cooperation diversity (UCD), has recently emerged smartly utilizing the concept of path diversity. The UCD scheme is based on the fundamental principle that wireless nodes exchange information and cooperatively transmit it to a shared destination. The UCD scheme results in higher data rates and better BER performance, in contrast to its non-cooperative counterpart scheme [19]. In this UCD technique, the cooperative user is typically known as a relay which usually uses various cooperative protocols [20], namely Amplify-and-Forward (AF) [21], Decode-and-Forward (DF) [22] or Compress-and-Forward (CF) [23], to accomplish the communication process.

Due to the deployment of extremely complicated equalizers, it has always been difficult to develop an efficient wideband wireless communication system which employs standard single-carrier (SC) modulation over frequency-selective Rayleigh fading (FSRF) channel [24]. Nevertheless, by using multi-carrier (MC) modulation, such as OFDM, this issue can be avoided. By successfully eliminating inter-symbol interference (ISI), OFDM is a wideband modulating and multiplexing technology which completely seizures the multipath energy. Thus, OFDM is qualified as an effective and renowned anti-multipath technique over FSRF channels [25]. OFDM is generally used in combination with Alamouti space-time block codes (STBCs), so that the transmitted STBC's inherent power can be effectively exploited over frequency-selective (FS) fading channels [26], [27]. The cooperative communication is generally employed with STBC to further utilize the additional spatial diversity which is generally called distributed space-time (ST) cooperative communication [28]. Distributing STBCs based on the OFDM system over FS channels resulted in cooperative diversity [29]. The channel

coding is frequently linked with a cooperative diversity scheme for utilizing the multipath diversity as well as spatial diversity which is also known as coded-cooperative diversity. Different channel codes are deployed in this diversity scheme, to effectively offer cooperative diversity. The authors Lin et al. in [30] have discussed coded-cooperative OFDM system that utilizes time division multiple access (TDMA) scheme. This TDMA technique is similar to the coded-cooperative methods already described such that all of the subcarriers in the first part of the codeword during time slot 1 are transmitted by each user. After the successful decoding of the data, the relay node sends all of the subcarriers in the second part of the codeword during time slot 2 over FS fading channels. OFDM effectively minimizes the impact of ISI and inter-carrier-interference (ICI), offering high spectral efficiency in wideband wireless communication.

For further improving the BER performance of an OFDM system, distributed channel codes can be used in the coded-cooperative scenario, providing temporal diversity [31]. Different types of distributed channel codes, namely convolution codes [32], [33], [34], LDPC codes [12], [35], [36], Turbo codes [17], [37], [38], Reed-Muller (RM) code [39], [40], [41] and more recently Polar codes [42], [43], [44] are already combined with OFDM system in coded-cooperative communication to efficiently provide the temporal diversity. The OFDM scheme combined with MIMO antennas has been very well-known for a couple of decades because it efficiently utilizes both frequency diversity as well as spatial diversity in FS MIMO channels. A number of researchers have concentrated their efforts on creating improved cooperative strategies incorporated with MIMO systems, to obtain an advantage in terms of both spatial as well as temporal diversities.

In wireless communication, using multiple transmit-antennas (TAs) and receive-antennas (RAs) to take advantage of multipath propagation, MIMO is a technique for increasing a radio link's capacity [37], [27]. By employing multiple antennas (MAs) at the transmitter and receiver, a MIMO system increases the performance and channel capacity of a wireless communication system. With the recent development of wireless communication technology, MIMO has become a crucial component of every latest communication standard. For example, Wi-Fi, 5G/6G mobile networks, IEEE 802.11n (Wi-Fi 4), IEEE 802.11ac (Wi-Fi 5), WiMAX, Long Term Evolution, LTE-Advanced and HSPA+(3G) make extensive use of MIMO technology. MIMO technology plays a significant role in the evolution of wireless communication systems, specifically for achieving higher data rates, improved spectral efficiency, and better reliability. The use of MAs allows for spatial diversity, spatial multiplexing, and advanced signal processing techniques to enhance the overall performance of the system.

In this paper, we have proposed an effective and competitive AJ technique based on the STC-OFDM scheme incorporated with Alamouti STBC-MIMO (2×2) antennas as an effective way to decrease the potential effect of wideband noise jamming. To the best of our knowledge, the STC-OFDM scheme incorporated with Alamouti STBC-MIMO (2×2) system in a non-cooperative as well as coded-cooperative wireless communication over an additive white Gaussian noise (AWGN) and a slow FSRF channels under wideband noise jamming environment has not been explored till date. This paper aims to investigate both the abovementioned scenarios and, therefore, investigating and addressing the stated issues is the major motivation and research impact of this manuscript. Almost all of the earlier published work regarding the TCS and STC-OFDM scheme over the AWGN channel or FSRF channel is without incorporating the OFDM scheme and STBC-MIMO system under the jamming environment [13], [14], [15]. The bit error performance of Turbo coded OFDM over AWGN and Rayleigh fading channels under various types of noises has been analyzed by the author Chronopoulos et al. in [45]. Thus, the existing research regarding Turbo codes under jamming attacks cannot be applied to any practical standard of wireless communication system. More specifically, distributed Turbo codes (DTCs) in cooperative communication over FSRF channels employing OFDM in combination with STBC-MIMO has not been explored to date under noise jamming attacks. Therefore, this article's main objective is to explore and analyze the BER performance of the STC-OFDM scheme with STBC-MIMO (2×2) antennas for coded-cooperative wireless communication over FSRF channels. To the far extent of our information, the closest work to this research paper is accomplished in [37], in which the bit error performance of a Turbo coded OFDM using matched interleaver combined with MIMO antennas for coded-cooperative wireless communication, has been investigated under non-jamming environment. Another work based on a distributed Polar coded OFDM system using Plotkin's construction with MIMO antennas under non-jamming environment which closely resembles to ours can be found in [46]. Although both the stated works consider the OFDM scheme incorporated with STBC-MIMO (2×2) antennas for coded-cooperative wireless communication over AWGN and FSRF channels, they do not investigate the bit error performance of the proposed schemes under the jamming environment. Furthermore, investigating and addressing these issues is the major contribution and incentive of this manuscript.

This research article claims the following three major novel contributions:

- The STC-OFDM scheme incorporated with Alamouti STBC-MIMO (2×2) antennas is proposed as an effective way to decrease the potential effect of wideband noise jamming and to prove that the STC-OFDM-MIMO system can work as a competitive AJ technique.
- The proposed STC-OFDM scheme with Alamouti STBC-MIMO (2×2) antennas is extended to a coded-cooperative wireless communication scenario and the BER performance of this distributed scheme is investigated for the first time under the noise jamming environment to the best of our knowledge.

- The bit error performance of a single-relay DSTC-OFDM-MIMO (coded-cooperative) scheme is compared with that of the STC-OFDM-MIMO (non-cooperative) scheme as a suitable benchmark, under the same conditions and the noise jamming environment.
- Both the proposed MIMO schemes are also compared with the corresponding single-antenna (SA) schemes, under the same conditions and the noise jamming environment.

The rest of this research article can be structured as under: In Sec. 2, the system description of the proposed STC-OFDM scheme incorporated with STBC-MIMO (2×2) antennas for the non-cooperative communication system is presented. In Sec. 3, the system description of the proposed DSTC-OFDM scheme incorporated with STBC-MIMO (2×2) antennas for the coded-cooperative communication system is discussed. Section 4 briefly describes the joint iterative SISO (JISISO) decoding technique which is particularly designed for the proposed DSTC-OFDM-MIMO scheme. Section 5 presents and discusses the simulation set-up along with the Monte Carlo simulation results for both the STC-OFDM-MIMO (non-cooperative) and DSTC-OFDM-MIMO (coded-cooperative) schemes with different jamming scenarios. Lastly, the paper is concluded in Sec. 6 with the conclusion drawn based on the observations and simulation results given in Sec. 5.

2. The Conventional STC-OFDM Scheme with STBC-MIMO (2×2) Antennas for Non-Cooperative Wireless Communication System under Noise Jamming Attack

In this section, a brief overview of the proposed STC-OFDM scheme with STBC-MIMO (2×2) antennas for a non-cooperative wireless communication system is presented and discussed, along with the details of the encoding and decoding processes. A typical symmetric TCS consists of two identical RSC encoders concatenated in parallel, with a random interleaver (RI), denoted by π and connected as depicted in Fig. 1, and a Turbo code decoder, comprising of two constituent iterative soft-input/soft-output (SISO) decoders. The TCS with parallel concatenation is represented by $\mathbf{C} = (C_1, C_2)$, where C_1 and C_2 denote identical encoders. In this manuscript, symmetric TCS having identical RSC encoders with constraint length $K_L = 3$ and overall code rate $R_c = 1/3$ is selected and investigated. Each encoder has the same generator matrix $\mathbf{G}(D) = [1, \mathbf{g}_2(D)/\mathbf{g}_1(D)]$, where $\mathbf{g}_1(D) = (1 + D + D^2)$ represents the feed-back polynomial and $\mathbf{g}_2(D) = (1 + D^2)$ represents the feed-forward polynomial with constraint length $K_L = 3$. The generator matrix $\mathbf{G}(D)$ of each encoder can also be represented in its equivalent octal form $\mathbf{G}(D) = (1,5/7)_8$. The STC system with overall generator matrix $\mathbf{G}(1,5/7,5/7)_8$ and the code rate $R_c = 1/3$ is considered

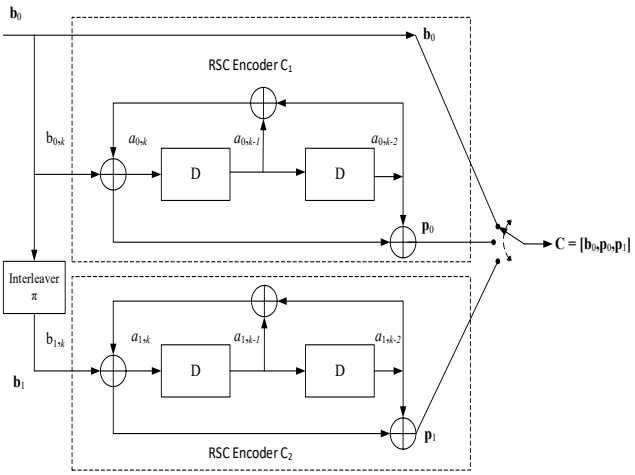

Fig. 1. A 1/3 code rate symmetric Turbo code encoder having generator matrix $\mathbf{G}(D) = (1,5/7,5/7)_8$ and constraint length $K_L = 3$.

and employed in the proposed AJ communication model because of its superior BER performance and robustness. The specific parameters $K_L = 3$ and $R_c = 1/3$ have been selected based on a balance between FEC performance and computational complexity, ensuring robust and efficient operation in practical communication systems. These choices support the overall objective of enhancing the reliability and efficiency of the symmetric TCS in our proposed scheme.

The schematic diagram of the proposed STC-OFDM scheme incorporated with STBC-MIMO (2×2) antennas for non-cooperative wireless communication system under the jamming environment is shown in Fig. 2. The information bits sequence $\mathbf{b}_0$ of frame length l is fed into an RSC encoder-1 (C_1) which generates the parity bits sequences $\mathbf{p}_0$. The same information bits sequence $\mathbf{b}_0$ is given as input to an RSC encoder-2 (C_2) simultaneously, after passing through a RI which generates parity bits sequence $\mathbf{p}_1$. The RI shuffles the sequence $\mathbf{b}_0$ in a random way to produce an interleaved sequence of information bits $\mathbf{b}_1 = \pi\mathbf{b}_0$. The sole purpose of this interleaving is the de-correlation of the original information bit sequence, which enables an iterative Turbo code decoding technique to be performed. The iterative Turbo code decoding technique is based on the exchange of extrinsic information (I_{Ext}) from one component SISO decoder to another in an iterative manner. Thus, the encoded Turbo code frames are made up of information bits $\mathbf{b}_0$ along with the two respective parity bits sequences $\mathbf{p}_0$ and $\mathbf{p}_1$. A mapper then maps this Turbo-encoded sequence of coded bit frame $\mathbf{s}$ to generate digitally modulated complex symbols $\mathbf{x}$, i.e., BPSK, 4-QAM or 16-QAM. Through Alamouti STBC encoding [27], two parallel encoded signals c_1 and c_2 are then obtained. At time instants $t_1 = n$ and $t_2 = (t_1 + T) = (n + 1)$ where T is the OFDM symbol time, (c_1, c_2) and $(-c_2^*, c_1^*)$ are transmitted via two parallel paths, respectively. Then, these two sequences of symbols are transformed from the frequency-domain into the time-domain by applying a K-point inverse discrete Fourier transform (K-IDFT) operation to the corresponding signals. The corresponding STBC-encoded OFDM symbols

are finally obtained by appending cyclic prefix (*CP*), which are then sent via the transmitting antennas T_{x_1} and T_{x_2} respectively over an FSRF channel **H**. The DFT has a well-known characteristic of producing multiplication in the frequency-domain from circular convolution in the time-domain. The channel entries are supposed to be unchanged for two successive Alamouti ST block codes and as a result, the channel is eligible to be known as a slow FSRF channel. Moreover, the receiver is fully aware of channel **H** entries, whereas the transmitter is unaware of the channel **H** entries. The coded symbol sequence $\mathbf{x} = [x_1, x_2,\ldots, x_k,\ldots, x_N]$ of length N, is generated by digitally modulating the Turbo-encoded bit sequence **s** of the same length N, where x_k represents the BPSK, binary 4-QAM or 16-QAM digital modulated symbol, such that $x_k \in \{-1, +1\}$, $x_k \in \{1+j, 1-j, -1+j, -1-j\}$ or $x_k \in \{-3-3j, -3-j, -3+3j, -3+j, -1-3j, -1-j, -1+3j, -1+j, 3-3j, 3-j, 3+3j, 3+j, 1-3j, 1-j, 1+3j, 1+j\}$ respectively. The coded sequence of symbols is divided into ($k\times1$) sized blocks, which can be expressed as under:

$$\mathbf{x}(n) = \left[\, x(nk)\ldots x(nk+k-1)\right]^{T}. \tag{1}$$

Every two consecutive blocks are transformed by the STBC encoder into the matrix $\mathbf{X}(n)$ of size $(k \times 1) + (k \times 1) = (2k \times 2)$, given by,

$$\mathbf{X}(n) = \begin{bmatrix} \mathbf{x}(2n) & -\mathbf{x}^{*}(2n+1) \\ \mathbf{x}(2n+1) & \mathbf{x}^{*}(2n) \end{bmatrix} \tag{2a}$$

where the rows (i.e., blocks) of the matrix are sent via the transmitting antennas T_{x_1} and T_{x_2}, respectively and the columns of the matrix are sent in two successive time slots, i.e., n and $n+1$. Thus, from the matrix $\mathbf{X}(n)$, the two codewords $\mathbf{c}(n)$ and $\mathbf{c}(n+1)$ are obtained, given as under:

$$\mathbf{X}(n) = \left[\mathbf{c}(n) \quad \mathbf{c}(n+1)\right] \tag{2b}$$

where $\mathbf{c}(n) = \begin{bmatrix} \mathbf{x}(2n) \\ \mathbf{x}(2n+1) \end{bmatrix}$, $\mathbf{c}(n+1) = \begin{bmatrix} -\mathbf{x}^{*}(2n+1) \\ \mathbf{x}^{*}(2n) \end{bmatrix}$.

Before transmitting the k-long symbols, we apply inverse fast Fourier transform (IFFT) operation and then, append the *CP*, to obtain the corresponding $\bar{p}\times1$ symbols. In one complete OFDM frame, the linear convolution is effectively transformed into the circular convolution, provided that the *CP* length (L_{CP}) exceeds the delay spread of the FS channel. This IFFT operation and *CP* component transform the FS fading channels into the frequency-flat fading channels, which enables us to effectively use the advantage of transmit diversity formed by the STBC encoder. Then, the two STBC-encoded OFDM symbols $\mathbf{c}(n)$ and $\mathbf{c}(n+1)$ are sent via the channels with an impulse response vector $\boldsymbol{h}_{j,m}^{p}$, where p defines the number of channel taps (i.e., $p = 0, 1,\ldots, P-1$), j represents the number of RAs and m represents the number of TAs, such that $m = [1, 2]$, $\boldsymbol{h}_{j,m}^{p} \neq 0 \,\forall\, p \in [0, P]$. The signal vector **y** received from the FSRF channel at the receiver, assumed for two successive channel usages, at time instants n and $n+1$, can be modeled as under:

$$\mathbf{y}(n) = \mathbf{H}^{p} \circledast \mathbf{c}(n) + \boldsymbol{w}(n), \tag{3a}$$

$$\mathbf{y}(n+1) = \mathbf{H}^{p} \circledast \mathbf{c}(n+1) + \boldsymbol{w}(n+1). \tag{3b}$$

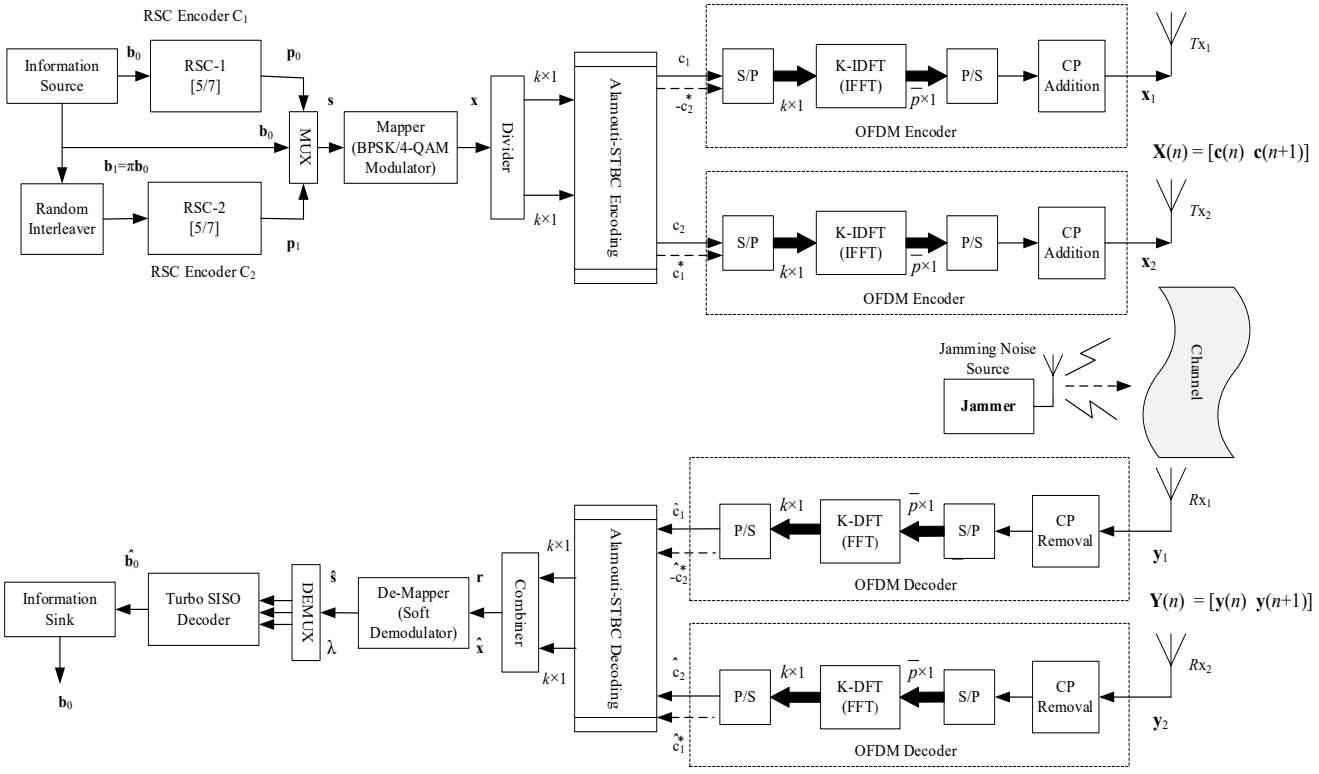

Fig. 2. Block diagram of the proposed STC-OFDM scheme with Alamouti STBC-MIMO (2×2) antennas.

Under the jamming signals $z^J(n)$ and $z^J(n+1)$ at time instants n and $n+1$ respectively,

$$\mathbf{y}(n) = \mathbf{H}^p \circledast \mathbf{c}(n) + \boldsymbol{w}(n) + \mathbf{G}\ z^J(n), \tag{4a}$$

$$\mathbf{y}(n+1) = \mathbf{H}^p \circledast \mathbf{c}(n+1) + \boldsymbol{w}(n+1) + \mathbf{G}\ z^J(n+1) \tag{4b}$$

$$\mathbf{H}^p = \begin{bmatrix} h_{11}^p & h_{12}^p \\ h_{21}^p & h_{22}^p \\ \vdots & \vdots \\ h_{i1}^p & h_{i2}^p \\ \vdots & \vdots \\ h_{j1}^p & h_{j2}^p \end{bmatrix}, \quad \mathbf{G} = \begin{bmatrix} g_1 \\ g_2 \\ \vdots \\ g_i \\ \vdots \\ g_j \end{bmatrix} \tag{5}$$

where '$\circledast$' is the discrete-time (DT) circular convolution operator, $\mathbf{H}^p$ is the time-domain FSRF channel with each vector $\boldsymbol{h}_{j,m}^p = [h_{j,m}^0, h_{j,m}^1, \ldots, h_{j,m}^i, \ldots, h_{j,m}^{P-1}]$ where $h_{j,m}^i$ is an independent and identically distributed (i.i.d.) complex Gaussian random variable having zero-mean and variance ½ per dimension. $\boldsymbol{w}(n)$ represents an uncorrelated complex-valued noise vector, such that $\boldsymbol{w}(n) = [w_1, w_2, w_3, \ldots, w_i, \ldots, w_q]$ whose element w_i is zero-mean complex Gaussian variable with independent real and imaginary parts of equal variances $N_0/2$, where N_0 is the noise power spectral density (PSD), and q denotes the number of noise coefficients, i.e., $q = P + CP + \mathrm{K} - 1$. The term $z^J(n)$ and $z^J(n+1)$ are defined as the jamming signals at time instants n and $n+1$ respectively. $\mathbf{G}$ is the time domain FSRF channel from the jammer J to the receiver R_x whose every entry is a vector g_i which is an i.i.d. complex Gaussian random variable, such that $\mathbf{G} = [g_1, g_2, g_3, \ldots, g_i, \ldots, g_j]^T$, where $g_i \sim R(0, \sigma_J^2)$, $(i = 1,2,3,\ldots..,j)$ with zero-mean and variance $\sigma_J^2 = J_0/2$ variance complex Gaussian random variable, where J_0 is the jamming PSD.

At the receiver, after removing the *CP* first and applying serial-to-parallel (*S/P*) conversion, the K-point FFT operation is applied to the corresponding sequence of coded symbols. Alamouti ST block decoding [27] is then applied in frequency-domain, after parallel-to-serial (*P/S*) conversion. The received sequence of symbols $\hat{\mathbf{x}} = \mathbf{r} = [\mathrm{r}_1, \mathrm{r}_2, \ldots, \mathrm{r}_k, \ldots, \mathrm{r}_N]$ is obtained, where k represents the time instant of $\mathbf{x}$. This received signal vector $\hat{\mathbf{x}}$ is passed through a digital soft-demodulator (de-mapper) to generate the log-likelihood ratios (*LLRs*) of each coded bits $\boldsymbol{\lambda} = [\lambda_1, \lambda_2, \lambda_3, \ldots, \lambda_N]$ [46]. These *LLRs* so obtained, are fed into Turbo code decoder, resulting in the estimated information bits sequence $\hat{\mathbf{b}}_0$, which can mathematically be expressed as under:

$$LLR\left(\mathrm{x}_k^{\bar{q}}\right) = \log \frac{P\left(\mathrm{x}_K^{\bar{q}} = 1 \mid r_k\right)}{P\left(\mathrm{x}_K^{\bar{q}} = 0 \mid r_k\right)}, \tag{6}$$

$$LLR\left(\mathrm{x}_k^{\bar{q}}\right) = \log \frac{\sum_{\mathrm{x}_k \in \varnothing_1^{\bar{q}}} P(r_k \mid \mathrm{x}_k) \prod_{\alpha=1}^{\beta} P\left(\mathrm{x}_k^{\alpha}\right)}{\sum_{\mathrm{x}_k \in \varnothing_0^{\bar{q}}} P(r_k \mid \mathrm{x}_k) \prod_{\alpha=1}^{\beta} P\left(\mathrm{x}_k^{\alpha}\right)}, \tag{7}$$

$$LLR\left(\mathrm{x}_k^{\bar{q}}\right) = \log \frac{\sum_{\mathrm{x}_k \in \varnothing_1^{\bar{q}}} \exp\left\{-\left(\left|r_k - \mathrm{x}_k\right|^2 + \prod_{\alpha=1}^{\beta} P\left(\mathrm{x}_k^{\alpha}\right)\right)\right\}}{\sum_{\mathrm{x}_k \in \varnothing_0^{\bar{q}}} \exp\left\{-\left(\left|r_k - \mathrm{x}_k\right|^2 + \prod_{\alpha=1}^{\beta} P\left(\mathrm{x}_k^{\alpha}\right)\right)\right\}} \tag{8}$$

where the bit position is defined by $\bar{q}$, such that $\bar{q} = [1,2]$, $\beta = \log_2 M$ and $\varnothing_0^{\bar{q}}, \varnothing_1^{\bar{q}}$ represents the vector of symbols taking a value of 0 or 1 at the $\bar{q}$-th bit respectively [46]. These *LLRs* are fed into the Turbo code decoder that eventually estimates the message sequence of bits $\hat{\mathbf{b}}_0$, which contains the original sequence of information bits $\mathbf{b}_0$.

3. The Distributed STC-OFDM Scheme with STBC-MIMO (2×2) Antennas for Coded-Cooperative Wireless Communication System under Noise Jamming Attack

This section presents and discusses the proposed single-relay DSTC-OFDM scheme with Alamouti STBC-MIMO (2×2) antennas for coded-cooperative wireless communication system, along with the details of the encoding and decoding processes. The TCS fits naturally well in a typical cooperative communication framework. Hence, the proposed MIMO scheme based on DTCs can efficiently be implemented in a coded-cooperative wireless communication system. An innovative concept of a three-terminal network proposed by Van Der Meulen in [47], serves as the foundation for our proposed MIMO scheme. A cooperative wireless communication model with a three-terminal network employing OFDM over FS fading channels is discussed in the literature [30], [37]. The three terminals considered are the source node *S*, the relay node *R*, and the destination node *D*. The way TCS is structured makes it highly appropriate to deploy in a coded-cooperative communication system where it is distributed over the source *S* and the relay *R* nodes in such a way that cooperation occurs between these two nodes. An important class of coded-cooperative communication is thus formed, which is generally referred to as DTCs [18], [37]. The schematic diagram of the proposed single-relay DSTC-OFDM scheme incorporated with STBC-MIMO (2×2) antennas for a coded-cooperative wireless communication system under the jamming environment is shown in Fig. 3.

The complete Turbo codeword is divided into two RSC codes. RSC encoder-1 (C_1) is located at the source node *S* and RSC encoder-2 (C_2) is located at the relay node *R*. The relay node *R* and the destination node *D* are placed close to each other. The entire transmission cycle of the information bits sequence $\mathbf{b}_0$ from the source node *S* to the destination node *D* is completed in two consecutive time slots. During time slot 1, the sequence of information bits $\mathbf{b}_0$ is encoded by the source node *S* using the RSC encoder C_1 to generate the codeword ($\mathbf{b}_0$,$\mathbf{p}_0$), where $\mathbf{p}_0$ is the parity bit sequence. After passing through a BPSK mapper the acquired codeword s^1 of length N_1 is passed through the

STBC-OFDM encoder, resulting in STBC-encoded OFDM symbols $\mathbf{c}_S$ (i.e., the first part of the codeword) being transmitted to both relay *R* and destination *D* nodes in the same time slot as illustrated in Fig. 3. The STBC-OFDM encoding process has already been described in the previous section of this paper. The relay node *R* receives the encoded sequence of symbols after the corresponding demodulation and then, it decodes the received sequence of information bits. This decoding is considered as ideal or perfect because the source-to-relay (*S*-*R*) channel is considered as ideal or error-free. The estimated information bits sequence $\mathbf{b}_0$ is delivered to a RI to generate an interleaved information bits sequence $\mathbf{b}_1 = \pi\mathbf{b}_0$, which is encoded by the relay node *R* using the RSC encoder C_2, to generate the parity bit sequence $\mathbf{p}_1$. In time slot 2, the relay node *R* retransmits the encoded sequence of symbols to the destination node *D* after modulation via the relay-to-destination (*R*-*D*) FSRF channel. Finally, a joint iterative Turbo code decoder decodes the signals received from the source *S* and relay *R* nodes, which is estimated by employing JISISO (Turbo) decoding technique at the destination node *D*.

During time slot 1, the relay node receives the signal vector $\mathbf{y}_{S–R}$ from the source node which can be modeled as under:

$$\mathbf{y}_{S-R}(n) = \mathbf{H}^{p}_{S-R} \circledast \mathbf{c}_S(n) + \boldsymbol{w}_{S-R}(n), \quad (9a)$$

$$\mathbf{y}_{S-R}(n+1) = \mathbf{H}^{p}_{S-R} \circledast \mathbf{c}_S(n+1) + \boldsymbol{w}_{S-R}(n+1). \quad (9b)$$

Under the jamming signals $z^{J1}(n)$ and $z^{J1}(n+1)$ at time instants *n* and *n*+ 1 respectively, during time slot 1,

$$\mathbf{y}_{S-R}(n) = \mathbf{H}^{p}_{S-R} \circledast \mathbf{c}_S(n) + \boldsymbol{w}_{S-R}(n) + \mathbf{G}_{J-R}\, z^{J1}(n) \quad (10a)$$

$$\mathbf{y}_{S-R}(n+1) = \mathbf{H}^{p}_{S-R} \circledast \mathbf{c}_S(n+1) + \boldsymbol{w}_{S-R}(n+1) + \mathbf{G}_{J-R}\, z^{J1}(n+1) \quad (10b)$$

where *n* and *n* + 1 denote two successive channel usages, $\circledast$ is the DT circular convolution operator, $\mathbf{H}^{p}_{S-R}$ represents the multipath FSRF channel from the source node to the relay node with multiple taps, such that $\mathbf{H}^{p}_{S-R} = \mathbf{H}^{p}_{j,m}$, where *p* defines the number of channel taps, (i.e., $p = 0, 1, \ldots, P-1$), *j* denotes the number of RAs and *m* denotes the number of TAs, such that $m = [1, 2]$, $\boldsymbol{h}^{p}_{j,m} \neq 0 \,\forall\, p \in [0, P]$. Every element of the matrix $\mathbf{H}^{p}_{j,m}$ represents a vector $\boldsymbol{h}^{p}_{j,m} = [h^{0}_{j,m}, h^{1}_{j,m}, \ldots, h^{i}_{j,m}, \ldots, h^{P-1}_{j,m}]$ where $h^{i}_{j,m}$ is an i.i.d. complex Gaussian random variable whose each component, i.e., in-phase and quadrature component, is zero-mean and variance ½. $\boldsymbol{w}_{S-R}$ is the noise vector, such that $\boldsymbol{w}_{S-R}(n) = [w_1, w_2, w_3, \ldots, w_i, \ldots, w_q]$ where w_i is a zero-mean complex Gaussian random variable with independent real and imaginary parts of equal variance $N_0/2$. The term $z^{J1}(n)$ and $z^{J1}(n+1)$ are the jamming signals during the first time slot, defined similarly as z^{J}. $\mathbf{G}_{J–R}$ is the time domain FSRF channel from the jammer *J* to the relay node *R* whose every entry is a vector g_i which is an i.i.d. complex Gaussian random variable, defined similarly as **G**. The channel from the source to the relay (*S*–*R*) is generally assumed to be ideal (i.e., SNR $\gamma_{S-R} = \infty$) to achieve perfect error-free decoding at the relay node. However, for a non-ideal *S*–*R* channel (i.e., SNR $\gamma_{S-R} \neq \infty$), various cooperative protocols have been discussed in the literature [32]. However, in this research study, the *S*–*R* channel is considered as ideal or perfect for the proposed model of coded-cooperative wireless communication. The entries of $\mathbf{H}^{p}_{S-D}$ fast-fading FSRF channel remains unchanged over the transmission of an entire STBC frame, i.e.,

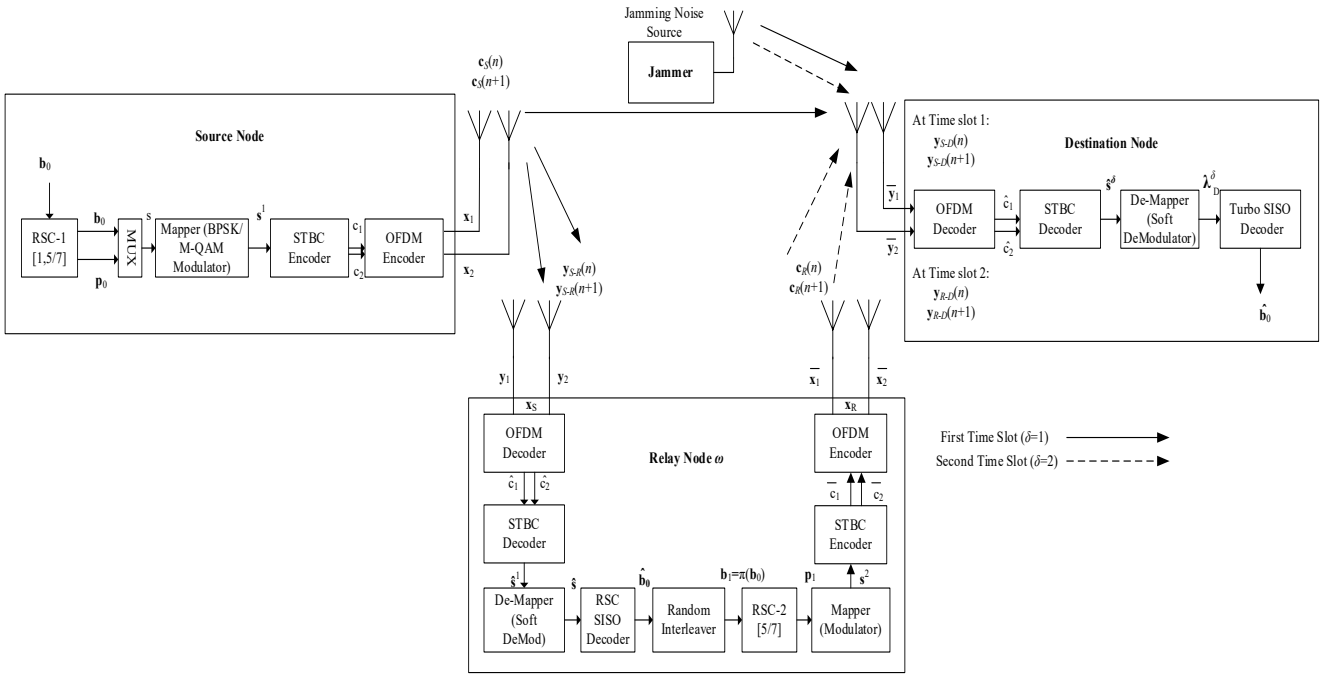

Fig. 3. Block diagram of the proposed DSTC-OFDM scheme with Alamouti STBC-MIMO (2×2) antennas.

$$\mathbf{H}_{S-D}^{p}=\left[\mathbf{H}_{S-D(1)}^{p},\mathbf{H}_{S-D(2)}^{p},\mathbf{H}_{S-D(3)}^{p},\ldots,\mathbf{H}_{S-D(N_1)}^{p}\right]. \quad (11a)$$

Nevertheless, for our proposed design, the entries of $\mathbf{H}_{S-D}^{p}$ FSRF channel stays constant over the transmission of a complete Turbo code frame, i.e.,

$$\mathbf{H}_{S-D}^{p}=\left[\mathbf{H}_{S-D(1)}^{p}=\mathbf{H}_{S-D(2)}^{p}=\ldots=\mathbf{H}_{S-D(N_1)}^{p}\right]. \quad (11b)$$

Thus, slow-fading is also incorporated into the proposed scheme over the FSRF channel. The STBC-encoded OFDM symbols $\mathbf{c}_S$ (i.e., the first part of the codeword) is broadcasted by the source node during time slot 1, the signal vector $\boldsymbol{y}_{S-D}$ received at the destination node, in the same time slot, can be modeled as under:

$$\mathbf{y}_{S-D}(n)=\mathbf{H}_{S-D}^{p}\circledast\mathbf{c}_S(n)+\boldsymbol{w}_{S-D}(n), \quad (12a)$$

$$\mathbf{y}_{S-D}(n+1)=\mathbf{H}_{S-D}^{p}\circledast\mathbf{c}_S(n+1)+\boldsymbol{w}_{S-D}(n+1). \quad (12b)$$

Under the jamming signals $z^{J1}(n)$ and $z^{J1}(n+1)$ at time instants n and $n+1$ respectively, during time slot 1,

$$\mathbf{y}_{S-D}(n)=\mathbf{H}_{S-D}^{p}\circledast\mathbf{c}_S(n)+\boldsymbol{w}_{S-D}(n)+\mathbf{G}_{J-D}z^{J1}(n), \quad (13a)$$

$$\mathbf{y}_{S-D}(n+1)=\mathbf{H}_{S-D}^{p}\circledast\mathbf{c}_S(n+1)+\boldsymbol{w}_{S-D}(n+1)+\mathbf{G}_{J-D}z^{J1}(n+1) \quad (13b)$$

where the matrix $\mathbf{H}_{S-D}^{p}$ denotes source-to-destination (S–D) FSRF channel and $\boldsymbol{w}_{S-D}$ is the noise vector, both of which are already defined likewise as $\mathbf{H}_{S-R}^{p}$ and $\boldsymbol{w}_{S-R}$ in (9). $\mathbf{G}_{J-D}$ is the time domain FSRF channel from the jammer J to the destination node D whose every entry is a vector $\boldsymbol{g}_i$ which is an i.i.d. complex Gaussian random variable, defined likewise as $\mathbf{G}$ The signal vector $\boldsymbol{y}_{S-D}$ received at the destination node is given as input to the STBC-OFDM decoder which generates the output symbol vector $\mathbf{Y}_1$ during time slot 1. The STBC-OFDM decoding process has already been described in the previous section of this paper.

The signal vector $\mathbf{y}_{S-R}$ received at the relay node, is fed into the STBC-OFDM decoder which generates the estimated coded sequence of soft-bits λ_{S-R}. This soft-bit coded sequence λ_{S-R} is then passed through a SISO decoder-1 (corresponding to RSC encoder C_1) to estimate $\hat{\mathbf{b}}_0$ information bits. During time slot 2, $\hat{\mathbf{b}}_0$ information bits are passed through a RI to obtain the interleaved sequence of information bits $\mathbf{b}_1$. This interleaved information bits sequence $\mathbf{b}_1$ is then further re-encoded using RSC encoder C_2 which generates the parity bit sequence $\mathbf{p}_1$ of length N_2. After passing through a BPSK mapper, this acquired codeword s^2 of length N_2 is fed into the STBC-OFDM encoder that generates the STBC-encoded OFDM symbols $\mathbf{c}_R$ (i.e., the second part of the codeword), being transmitted to the destination node in the second time slot as illustrated in Fig. 3. During time slot 2, the destination node receives the signal vector $\mathbf{y}_{R-D}$ from the relay node which can be modeled as under:

$$\mathbf{y}_{R-D}(n)=\mathbf{H}_{R-D}^{p}\circledast\mathbf{c}_R(n)+\boldsymbol{w}_{R-D}(n), \quad (14a)$$

$$\mathbf{y}_{R-D}(n+1)=\mathbf{H}_{R-D}^{p}\circledast\mathbf{c}_R(n+1)+\boldsymbol{w}_{R-D}(n+1). \quad (14b)$$

Under the jamming signals $z^{J2}(n)$ and $z^{J2}(n+1)$ at time instants n and $n+1$ respectively, during time slot 2,

$$\mathbf{y}_{R-D}(n)=\mathbf{H}_{R-D}^{p}\circledast\mathbf{c}_R(n)+\boldsymbol{w}_{R-D}(n)+\mathbf{G}_{J-D}z^{J2}(n), \quad (15a)$$

$$\mathbf{y}_{R-D}(n+1)=\mathbf{H}_{R-D}^{p}\circledast\mathbf{c}_R(n+1)+\boldsymbol{w}_{R-D}(n+1)+\mathbf{G}_{J-D}z^{J2}(n+1) \quad (15b)$$

where $\mathbf{H}_{R-D}^{p}$ and $\boldsymbol{w}_{R-D}$ are already defined similarly as in (9). Since the channel $\mathbf{H}_{R-D}^{p}$ remains constant over the transmission of one complete Turbo code frame, i.e.,

$$\mathbf{H}_{R-D}^{p}=\left[\mathbf{H}_{R-D(1)}^{p}=\mathbf{H}_{R-D(2)}^{p}=\ldots=\mathbf{H}_{R-D(N_1)}^{p}\right]. \quad (16)$$

The term $z^{J2}(n)$ and $z^{J2}(n+1)$ are the jamming signals during the second time slot, defined likewise as z^{J}. The signal vector $\mathbf{y}_{R-D}$ received at the destination node, is fed into STBC-OFDM decoder which generates the output symbol vector $\mathbf{Y}_2$ during time slot 2.

The $\mathbf{Y}_1$ codeword (i.e., RSC-1 encoded OFDM codeword) is transmitted by the source node S in time slot 1 to the SISO decoder-1 which corresponds to the RSC-1 encoder at the source node S. The $\mathbf{Y}_2$ codeword (i.e., RSC-2 encoded OFDM codeword) is transmitted by the relay node R in time slot 2 to the SISO decoder-2 which corresponds to the RSC-2 encoder at the relay node R. Finally, the combined signal vector $\mathbf{Y}$ received at the destination node D is obtained by concatenating the symbol vectors $\mathbf{Y}_1$ and $\mathbf{Y}_2$, received from the source node S and the relay node R, respectively. The overall vector $\mathbf{Y}$, which is the complete codeword bits reaching the destination node during one complete transmission cycle, can mathematically be expressed as under:

$$\mathbf{Y}=\left[\mathbf{Y}_2,\mathbf{Y}_1\right]. \quad (17)$$

This vector $\mathbf{Y}$ is finally fed into the joint iterative SISO (Turbo) decoder, explained in the subsequent section, to estimate the original message bits sequence $\hat{\mathbf{b}}_0$.

4. JISISO (Turbo) Decoding Technique for the Proposed DSTC-OFDM-MIMO Scheme

Another prominent and distinctive characteristic of the proposed single-relay DSTC-OFDM scheme incorporated with the STBC-MIMO (2×2) system for coded-cooperative wireless communication is the joint iterative SISO (Turbo) decoding technique. This JISISO Turbo code decoder for the proposed DSTC-OFDM-MIMO scheme, depicted in Fig. 4, is implemented in the destination node, utilizing two SISO modules for joint iterative decoding

operation. The SISO APP modules with both serial and parallel concatenation of Turbo codes for the iterative decoding are described by Benedetto et al. [48]. In a characteristic communications receiver, a demodulator generally generates soft decisions that are then fed into the soft-input/hard-output decoder, where the output of the decoder results in bits (i.e., hard decisions) after the final decoding process. However, a hard-output decoder is not suitable in a typical TCS, in which multiple component RSC encoders are employed. The Turbo code decoding process of TCS consists of feeding the outputs in an iterative manner from one decoder back to the inputs of another decoder. This is due to giving hard decisions as input to a decoder degrades the system performance as compared to soft decisions. Thus, a SISO decoder is required for the decoding of Turbo codes [7]. For the first decoding iteration of the SISO decoder, the binary data is usually considered to be equally probable which gives an initial a-priori *LLR* value. In the iterative decoding process, the extrinsic likelihood is fed back to the decoder input, which leads to refining the a-priori probability of the data for the subsequent iteration.

The design of the Turbo code decoder has been discussed in the literature [18] which mainly consists of two SISO decoders, corresponding to each RSC encoder. It has three separate inputs and a single output. The a-priori probabilities of systematic bits $\lambda_{\mathbf{b}_0}$, as well as parity bits $\lambda_{\mathbf{p}_0}$ and $\lambda_{\mathbf{p}_1}$, are fed into the SISO decoders, resulting in the output known as I_{Ext}. Three LLRs are accepted by each SISO decoder as inputs, to produce a single output. The LLRs of the information bits, LLRs of the parity bits, and LLRs of a-priori information bits constitute the SISO decoder's input, which generates I_{Ext} as its output for the systematic bits as well as parity bits. During time slot 1, the first soft-demodulator generates the LLRs λ_{D}^1 as an output which are soft-demodulated sequences of bits. This corresponds to the combined sequence of information bits and parity bits, after the Alamouti STBC and OFDM encoding, originated by the RSC encoder-1 at the source node *S*. The LLRs λ_{D}^1 is then divided by the de-multiplexer into two separate streams of bits, i.e., the information bits LLRs sequence $\lambda_{\mathbf{b}_0}^1$ and the parity bits LLRs sequence $\lambda_{\mathbf{p}_0}^1$. These LLRs are given as inputs to SISO decoder-1 which generates I_{Ext} for systematic bit sequence $\mathbf{D}_{\mathbf{b}_{12}}$ and for parity bit sequence $\mathbf{D}_{\mathbf{p}_0}$. The I_{Ext} sequence of systematic bits $\mathbf{D}_{\mathbf{b}_{12}}$ is passed through a RI, to get the interleaved I_{Ext} sequence of systematic bits $\bar{\mathbf{D}}_{\mathbf{b}_{12}} = \pi(\mathbf{D}_{\mathbf{b}_{12}})$, which is fed as an a-priori input into SISO decoder-2, while the I_{Ext} sequence of parity bits $\mathbf{D}_{\mathbf{p}_0}$ is discarded.

During time slot 2, the second soft-demodulator produces the LLRs $\lambda_{\text{D}}^2 = \lambda_{\mathbf{p}_1}^2$ as an output, which is the soft-demodulated sequence of bits. This corresponds to the sequence of parity bits $\mathbf{p}_1$, after the Alamouti STBC and OFDM encoding, transmitted by the RSC encoder-2 at the relay node *R*. The SISO decoder-2 produces I_{Ext} $\bar{\mathbf{D}}_{\mathbf{b}_{21}}$ and

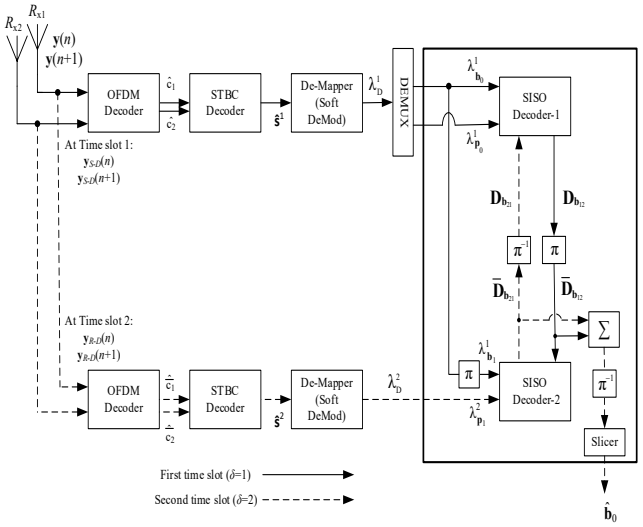

Fig. 4. JISISO (Turbo) decoding technique for the proposed DSTC-OFDM scheme with STBC-MIMO (2×2) antennas.

$\bar{\mathbf{D}}_{\mathbf{p}_1}$ that corresponds to the interleaved sequences of information bits $\mathbf{b}_1 = \pi\mathbf{b}_0$ and parity bits $\mathbf{p}_1$, respectively. The I_{Ext} $\bar{\mathbf{D}}_{\mathbf{b}_{21}}$ of interleaved information bits sequence $\mathbf{b}_1$ is de-interleaved to obtain $\mathbf{D}_{\mathbf{b}_{21}}$, which is then sent back to SISO decoder-1, whereas the I_{Ext} of parity bits sequence $\bar{\mathbf{D}}_{\mathbf{p}_1}$ is discarded. The two component SISO decoders exchange these I_{Ext} sequences $\mathbf{D}_{\mathbf{b}_{12}}$ and $\mathbf{D}_{\mathbf{b}_{21}}$ of corresponding message bits for a predefined number of iterations. The interleaved I_{Ext} $\bar{\mathbf{D}}_{\mathbf{b}_{12}}$ and $\bar{\mathbf{D}}_{\mathbf{b}_{21}}$ are then summed up in an adder, and de-interleaved after passing through a de-interleaver, which is then followed by a slicer. Finally, the hard decoding operation is performed by the slicer to obtain the estimated information bits sequence $\hat{\mathbf{b}}_0$ through which the complete decoding process of the transmitted information bits sequence $\mathbf{b}_0$ is accomplished.

5. Simulation Set-up and Results Discussion

In this section, the BER performances and simulation results of the proposed STC-OFDM-MIMO (non-cooperative) scheme and the DSTC-OFDM-MIMO (coded-cooperative) scheme are presented and discussed. The simulation tool, modulation technique and decoding algorithm employed for both the STC-OFDM-MIMO and DSTC-OFDM-MIMO schemes are MATLAB, BPSK/M-QAM modulation, and Log-MAP algorithm respectively. Both of the proposed MIMO schemes have been investigated and analyzed over the AWGN channel as well as the FSRF (slow) channel under the same wideband noise jamming environment and identical conditions i.e., the same overall code rate and data frame length of $R_{\text{c}} = 1/3$ and $l = 512$ bits respectively. The generator matrix for both the schemes is $\mathbf{G}(1,5/7,\ 5/7)_8$ having the length of RI equal to

the frame length l = 512 bits. The STC-OFDM-MIMO and DSTC-OFDM-MIMO schemes are simulated over AWGN, single-path as well as multipath FSRF channels. In addition, the proposed DSTC-OFDM-MIMO scheme can achieve both the cooperative diversity gain as well as the coding gain. The jamming signal can mathematically be represented as a wideband or broad-spectrum Gaussian noise for a fixed jammer received power J, with uncorrelated zero-mean and a flat PSD over the BW under consideration. When the jammer's tactic is to jam the entire frequency-range of interest W_B, this jammer is termed as a wideband noise or barrage jammer, and $J_0 = (J/W_B)$ is the jamming PSD [7]. However, in addition to white noise, the source of jamming, in this case, is considered as broadband Gaussian noise power from the jammer. Therefore, the SNR of interest can be written as $\gamma = [E_b/(N_0 + J_0)]$, where E_b represents the bit energy and J denotes the average jammer power received by the receiver. Since the jammer PSD is usually far larger than the noise PSD*, i.e.,* $J_0 >> N_0$, the typical SNR in a jamming environment is generally considered to be $\gamma = E_b/J_0$. Thus, $\gamma_{reqd.}$ is defined as the bit energy per jammer PSD, needed to maintain the communication link for a definite BER [7], which can mathematically be expressed as under:

$$\gamma_{\text{reqd.}} = \left(\frac{E_b}{J_0}\right)_{\text{reqd.}} = \frac{\left(W_B/\bar{R}\right)}{\left(\text{J/S}\right)_{\text{reqd.}}} = \frac{G_p}{\left(\text{J/S}\right)_{\text{reqd.}}} \tag{18}$$

where $E_b = ST_b = S/\bar{R}$, S is the received signal power, T_b is the bit duration, $\bar{R}$ is the data rate in bits/s and $G_p = W_B/\bar{R}$ represents the processing gain [7]. Therefore,

$$\left(\frac{J}{S}\right)_{\text{reqd.}} = \frac{G_p}{\left(E_b/J_0\right)_{\text{reqd.}}}. \tag{19}$$

The parameter $(J/S)_{reqd.}$ is the required ratio of jamming power to signal power, which defines a figure-of-merit to measure the robustness and invulnerability of a system to interference. For further details on the subject of jamming and the parameters of the threat model assumed, interested reader may refer to the reference [7].

In this paper, we have modeled the impact of wideband noise jamming by employing the noise parameter jamming-to-signal (J/S) ratio [7], which is primarily used to model the effect of the noise source. This J/S parameter may affect the received signal, while processing the genuine signal and is utilized in the SNR calculation (i.e., $\gamma_{reqd.}$) to define the signal quality as shown in (18). We have used a jamming source with a SA to generate random pseudo-noise (PN) sequence to jam the receiver R_x or the destination node D as defined in (4) and (13) respectively. The J/S ratio is normally taken to be 23 dB for noise jamming with the processing gain of $G_P = 1000$ [49], [50]. While implementing the worst-case jamming scenario, we have varied the intensity of wideband constant jamming signals to simulate three different levels of adversarial attack (i.e., J/S = 13 dB, 23 dB and 33 dB) over multipath FSRF (slow-fading) channel. The jamming scenario with J/S = 33dB is the worst-case jamming scenario for both the proposed schemes where the jammer operates at the highest possible power, utilizes advanced DSP techniques, and covers the full frequency spectrum of the target's operational frequencies [50].

Furthermore, the AJ strategies offered by the simulation results, so obtained from this research study, are not optimal for covering all possible aspects of jamming attacks. Certain aspects of jamming signals, including the temporal and frequency patterns, can be optimized, and then those sensitive components of the wireless communication system that are more vulnerable to jamming attacks are optimally selected [3]. In this research, however, the prime focus is given only on the relatively under-investigated class of the jamming attack, namely wideband Gaussian noise jamming, and provides specific insight on how to counter the potential effect of the wideband noise jamming attack. Wideband noise jamming attacks can have significant detrimental effects on a wireless communication system's performance by introducing significant interference across a wide frequency band, making it more challenging for the receiver to correctly decode the transmitted signals. The primary impacts of wideband jamming include an increased BER and degraded SNR which, in turn, increases packet loss and reduces the effective data rate respectively. For further details on the parameters of the threat model assumed, the reader may refer to the literature [7], [49]. The nominal data rates (R_{nom}) for the proposed schemes using different modulation techniques, namely BPSK, 4-QAM and 16-QAM, with bits per symbol 1, 2 and 4 are calculated to be 4.333, 8.667 and 17.333 Mbps respectively, without jamming. However, under the jamming environment, these data rates are reduced to a lower level depending on the intensity of the jamming signal. Under the wideband noise jamming scenario with an SNR of 0 dB (i.e., normalized signal power of 1) and a code rate of $R_c = 1/3$, the effective data rates (R_{eff}) for BPSK, 4-QAM and 16-QAM are calculated to be 3.991, 7.289 and 13.416 Mbps respectively, by considering the probability of successful transmission (1 – BER), i.e.,

$$R_{\text{eff}} = R_{\text{nom}}\left(1 - \text{BER}\right). \tag{20}$$

In this research study, the channels *S–D* and *R–D* are considered to be multipath FSRF channels which are statistically independent and modeled by the Monte Carlo method with 9 taps each [24], [25]. However, for all simulations in the coded-cooperative scenario, the *S–R* channel is supposed as ideal or perfect (i.e., SNR $\gamma_{S-R} = \infty$). This hypothesis is valid due to the fact that the DF cooperative protocol is applicable only when the *S–D* channel is severely degraded as compared to the *S–R* channel [22].

The complete list of parameters with specifications used in the simulation is summarized in Tab. 1.

For the multipath FSRF channels between different links, the delay spread is considered to be 9 bits and the phase of each path is evenly distributed between 0 and 2π radians [51]. The length of IFFT and *CP* is selected to be

Parameters	Specification
Modulation techniques	BPSK
	M-QAM
Multiplexing scheme	OFDM
FFT length (K)	64 bits
Number of data subcarriers	52
CP length (L_{CP})	16 bits
OFDM symbol size	64 + 16 = 80 bits
FFT sampling frequency	20 MHz [–10 MHz to +10 MHz]
Subcarrier spacing	312.5 kHz
Used subcarrier index	{–26 to –1, +1 to +26}
CP duration (T_{CP})	0.8 μs
OFDM data symbol duration (T_d)	3.2 μs
OFDM symbol duration (T_s)	4 μs
OFDM symbol rate ($1/T_s$)	250 ksymbols/sec
Channel models	AWGN, FSRF
Delay spread of a channel	9 bits
Multipath taps	9 taps
Multipath phase-shift	0–2π radians
Additional relay gain	+3 dB
Channel coding	Turbo codes
Generator polynomial for TCS	$(1,5/7,5/7)_8$
Data frame length (l)	512 bits
Turbo code frame length	512 × 3 = 1536 bits
Number of frames	100,000
Code rate (R_c)	1/3
Decoding technique	JISISO - Turbo
Decoding algorithm	Log-MAP
Log-MAP iterations	5
J/S ratio	23 dB
Processing gain (G_P)	1000

Tab. 1. List of the simulation parameters.

64 and 16 bits respectively, based on the IEEE 802.11a specifications for a wireless communication link built using OFDM [52]. The 802.11a standard for wireless local area (WLAN) networking operates in the 5 GHz frequency band and specifies multiple non-overlapping channels, each with a width of 20 MHz, within the 5 GHz range which are spread apart to reduce interference [52]. Moreover, in the context of 802.11a which uses OFDM, the effects of the Rayleigh fading channel are particularly relevant, capturing the random and time-varying characteristics of multipath fading.

A 2×2 MIMO system with Alamouti STBC provides a balanced approach with several advantages, particularly for applications requiring simplicity, cost-effectiveness, and energy efficiency as compared to massive MIMO technology. The choice between the two should be guided by the specific requirements of the AJ application, taking into account factors such as deployment environment, budget, and performance needs. The transitioning from a 2×2 MIMO system to a massive MIMO system can significantly enhance the performance and robustness of AJ systems against wideband jamming attacks through spatial diversity, multiplexing gain, enhanced signal processing techniques, and increased degrees of freedom [53]. However, this enhanced system's performance and resilience against wideband jamming attempts can be traded off at the cost of increased hardware complexity and computational power. In addition, careful consideration of implementation challenges and system integration is necessary to fully realize these benefits.

5.1 Performance Comparison between the STC-OFDM-MIMO (Non-Cooperative) Scheme and the DSTC-OFDM-MIMO (Coded-Cooperative) Scheme with and without Jamming over AWGN Channel

In this subsection, we present the BER performance comparison of the STC-OFDM-MIMO scheme for non-cooperative communication and the DSTC-OFDM-MIMO scheme for coded-cooperative communication over AWGN channel under non-jamming and jamming environments, as shown in Fig. 5(a). The simulation results reveal that the DSTC-OFDM-MIMO scheme outperforms the STC-OFDM-MIMO scheme over the AWGN channel with the BPSK modulation technique under both non-jamming and jamming environments for the entire SNR range under consideration. The BER curves also show that the performance gain of the DSTC-OFDM-MIMO scheme at BER $\approx 3 \times 10^{-6}$ over the STC-OFDM-MIMO scheme is 0.5 dB without jamming. Furthermore, the BER curve with jamming J/S = 23 dB shows that the performance gain of the DSTC-OFDM-MIMO scheme at BER $\approx 3 \times 10^{-6}$, over the STC-OFDM-MIMO scheme is 0.3 dB. The better performance of the DSTC-OFDM-MIMO scheme over the STC-OFDM-MIMO scheme is due to the path diversity provided by the relay node.

We have also compared the bit error performance of both the proposed MIMO schemes with that of the corresponding SA schemes over the AWGN channel. The simulation results reveal that the STC-OFDM-MIMO and DSTC-OFDM-MIMO schemes outperform the STC-OFDM-SA and DSTC-OFDM-SA schemes over AWGN channel with BPSK modulation technique under both non-jamming and different jamming environments for the entire SNR range under consideration. The BER curves also show that the performance gain of the STC-OFDM-MIMO and DSTC-OFDM-MIMO schemes at BER $\approx 3 \times 10^{-6}$ over the STC-OFDM-SA and DSTC-OFDM-SA schemes is 1.2 dB and 0.8 dB without jamming respectively. Moreover, the BER curves with jamming J/S = 23 dB show that the performance gain of the STC-OFDM-MIMO and DSTC-OFDM-MIMO schemes at BER $\approx 1 \times 10^{-5}$ over the STC-OFDM-SA and DSTC-OFDM-SA schemes is 1.1 dB and 0.7 dB respectively. Furthermore, the performance of the STC-OFDM-SA scheme with jamming J/S = 23 dB is the worst among all the compared schemes over an AWGN channel.

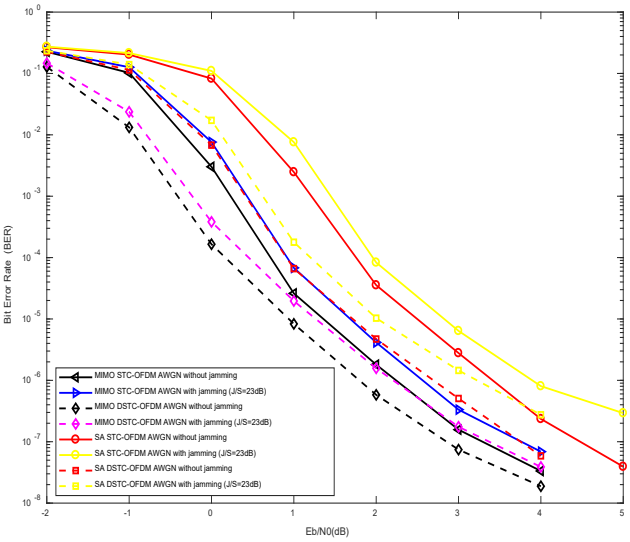

Fig. 5(a). The BER performances of the STC-OFDM-MIMO (Non-cooperative) scheme and the DSTC-OFDM-MIMO (Coded-cooperative) scheme over AWGN channel, with BPSK modulation technique, frame length $l = 512$, No. of frames = 100000 and 5 decoding iterations.

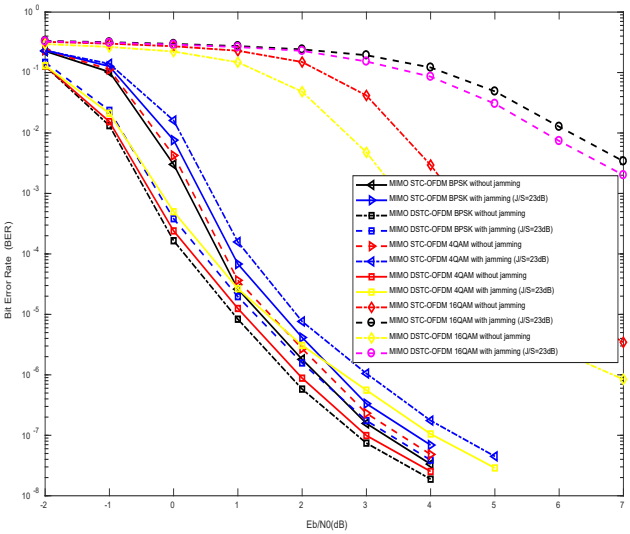

Fig. 5(b). The BER performances of the STC-OFDM-MIMO (Non-cooperative) scheme and the DSTC-OFDM-MIMO (Coded-cooperative) scheme over AWGN channel, with different modulation techniques (BPSK, 4-QAM and 16-QAM), frame length $l = 512$, No. of frames = 100000 and 5 decoding iterations.

In Fig. 5(b) the BER performance comparison of the STC-OFDM-MIMO scheme for non-cooperative communication and the DSTC-OFDM-MIMO scheme for coded-cooperative communication is presented over the AWGN channel under non-jamming and jamming environments with different modulation techniques, namely BPSK, 4-QAM and 16-QAM. The simulation results reveal that the BPSK modulation technique performs better in terms of BER for both the STC-OFDM-MIMO and DSTC-OFDM-MIMO schemes. However, in terms of BW efficiency, the 16-QAM modulation technique is better as compared to BPSK and 4-QAM modulation techniques. Furthermore, the performance of the STC-OFDM-MIMO scheme with 16-QAM modulation technique and jamming J/S = 23 dB, is the worst among all the compared schemes over an AWGN channel.

5.2 Performance Comparison between the STC-OFDM-MIMO (Non-Cooperative) Scheme and the DSTC-OFDM-MIMO (Coded-Cooperative) Scheme with and without Jamming over Single-path Fast FSRF Channel

This subsection presents the BER performance comparison of the STC-OFDM-MIMO scheme for non-cooperative communication and the DSTC-OFDM-MIMO scheme for coded-cooperative communication over single-path fast FSRF channel under non-jamming and jamming environments, as shown in Fig. 6. The simulation results show that in the low SNR region, the STC-OFDM-MIMO scheme performs almost similar to the DSTC-OFDM-MIMO scheme, however, in the high SNR region the DSTC-OFDM-MIMO scheme outperforms the STC-OFDM-MIMO scheme by a gain of 0.5 dB at BER $\approx 1 \times 10^{-5}$ over single-path FSRF (fast-fading) channel without jamming. Similarly, the DSTC-OFDM-MIMO scheme outperforms the STC-OFDM-MIMO scheme by a gain of 0.5 dB at BER $\approx 1 \times 10^{-5}$ over the aforementioned channel with jamming J/S = 23 dB.

We have also compared the bit error performance of both the proposed MIMO schemes with that of the corresponding SA schemes over a single-path fast FSRF channel. The simulation results reveal that the STC-OFDM-MIMO and DSTC-OFDM-MIMO schemes clearly outperform the STC-OFDM-SA and DSTC-OFDM-SA schemes

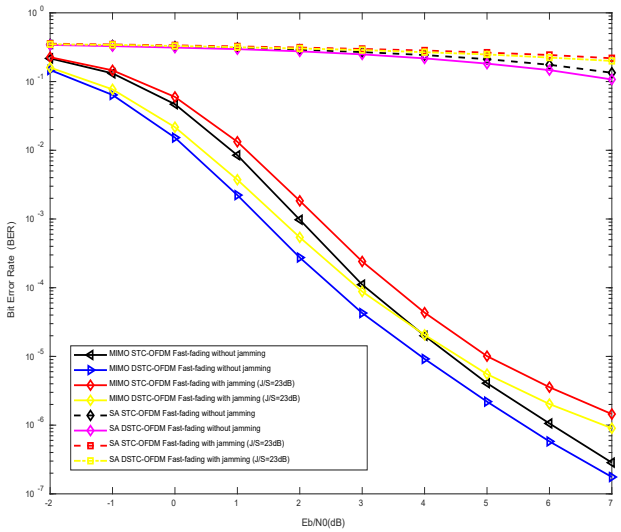

Fig. 6. The BER performances of the STC-OFDM-MIMO (Non-cooperative) scheme and the DSTC-OFDM-MIMO (Coded-cooperative) scheme over single-path fast FSRF channel, with BPSK modulation technique, frame length $l = 512$, No. of frames = 100000 and 5 decoding iterations.

by a significant margin over single-path fast FSRF channel with BPSK modulation technique under both non-jamming and jamming environments for the entire SNR range under consideration. The BER curves show that the BER performance of STC-OFDM-SA and STC-OFDM-MIMO schemes both at the SNR of 3 dB without jamming is 2.5×10^{-1} and 1.2×10^{-4} respectively. Moreover, the BER performance of STC-OFDM-SA and STC-OFDM-MIMO schemes both at the SNR of 3 dB with jamming J/S = 23 dB is 3×10^{-1} and 2.5×10^{-4} respectively. It is also observed from the BER curves that the BER performance of DSTC-OFDM-SA and DSTC-OFDM-MIMO schemes both at the SNR of 3 dB without jamming is 2×10^{-1} and 4×10^{-5} respectively. Moreover, the BER performance of DSTC-OFDM-SA and DSTC-OFDM-MIMO schemes both at the SNR of 3 dB with jamming J/S = 23 dB is 3×10^{-1} and 9×10^{-5} respectively. Furthermore, it is evident from the simulation results that the performance of the STC-OFDM-SA scheme with jamming J/S = 23 dB, is the worst among all the compared schemes over a single-path FSRF (fast-fading) channel.

5.3 Performance Comparison between the STC-OFDM-MIMO (Non-Cooperative) Scheme and the DSTC-OFDM-MIMO (Coded-Cooperative) Scheme with and without Jamming over Single-path Slow FSRF Channel

This subsection presents the BER performance comparison of the STC-OFDM-MIMO scheme for non-cooperative communication and the DSTC-OFDM-MIMO scheme for coded-cooperative communication over single-path slow FSRF channel under non-jamming and jamming environments, as shown in Fig. 7. The simulation results show that in the low SNR region, the STC-OFDM-MIMO scheme performs almost similar to the DSTC-OFDM-MIMO scheme, however, in the high SNR region the DSTC-OFDM-MIMO scheme outperforms the STC-OFDM-MIMO scheme by a gain of almost 4 dB at BER $\approx 2 \times 10^{-4}$ over single-path FSRF (slow-fading) channel without jamming. Similarly, the DSTC-OFDM-MIMO scheme outperforms the STC-OFDM-MIMO scheme by a gain of almost 6 dB at BER $\approx 2 \times 10^{-4}$ over the aforementioned channel with jamming J/S = 23 dB.

We have also compared the bit error performance of both the proposed MIMO schemes with that of the corresponding SA schemes over a single-path slow FSRF channel. The simulation results reveal that the STC-OFDM-MIMO and DSTC-OFDM-MIMO schemes clearly outperform the STC-OFDM-SA and DSTC-OFDM-SA schemes by a significant margin over single-path slow FSRF channel with BPSK modulation technique under both non-jamming and jamming environments for the entire SNR range under consideration. The BER curves show that the BER performance of STC-OFDM-SA and STC-OFDM-MIMO schemes both at the SNR of 10 dB without jamming is 5×10^{-2} and 2×10^{-4} respectively. Moreover, the

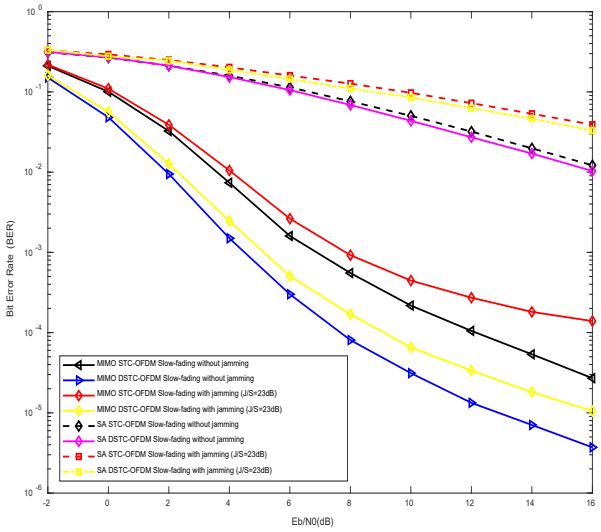

Fig. 7. The BER performances of the STC-OFDM-MIMO (Non-cooperative) scheme and the DSTC-OFDM-MIMO (Coded-cooperative) scheme over single-path slow FSRF channel, with BPSK modulation technique, frame length $l = 512$, No. of frames = 100000 and 5 decoding iterations.

BER performance of STC-OFDM-SA and STC-OFDM-MIMO schemes both at the SNR of 10 dB with jamming J/S = 23 dB is 1×10^{-1} and 4.5×10^{-4} respectively. It is also observed from the BER curves that the BER performance of DSTC-OFDM-SA and DSTC-OFDM-MIMO schemes both at the SNR of 10 dB without jamming is 4×10^{-2} and 3×10^{-5} respectively. Moreover, the BER performance of DSTC-OFDM-SA and DSTC-OFDM-MIMO schemes both at the SNR of 10 dB with jamming J/S = 23 dB is 9×10^{-1} and 7×10^{-5} respectively. Furthermore, it is evident from the simulation results that the performance of the STC-OFDM-SA scheme with jamming J/S = 23 dB, is the worst among all the compared schemes over a single-path FSRF (slow-fading) channel.

5.4 Performance Comparison between the STC-OFDM-MIMO (Non-Cooperative) Scheme and the DSTC-OFDM-MIMO (Coded-Cooperative) Scheme with and without Jamming over Multipath FSRF Channel

This subsection presents the BER performance comparison of the STC-OFDM-MIMO scheme for non-cooperative communication and the DSTC-OFDM-MIMO scheme for coded-cooperative communication over multipath FSRF channel with 9 taps under non-jamming and jamming environment, as shown in Fig. 8. The simulation results show that in the low SNR region, the STC-OFDM-MIMO scheme performs almost similarly to the DSTC-OFDM-MIMO scheme, however, in the high SNR region the DSTC-OFDM-MIMO scheme outperforms the STC-OFDM-MIMO scheme by a gain of 0.5 dB at BER $\approx 1 \times 10^{-5}$ over multipath FSRF channel without jamming. Similarly, the DSTC-OFDM-MIMO scheme

outperforms the STC-OFDM-MIMO scheme by a gain of 0.6 dB at BER ≈ 2×10^{-5} over multipath FSRF channel for both jamming scenarios, i.e., J/S = 13 dB and 23 dB. For the worst-case jamming scenario, we have considered a wideband constant jamming source with the intensity of jamming signals to simulate the highest level of adversarial attack (i.e., J/S = 33 dB) over multipath FSRF (slow-fading) channel [50]. Under this worst-case jamming scenario with jamming J/S = 33 dB, the DSTC-OFDM-MIMO scheme outperforms the STC-OFDM-MIMO scheme by a gain of 0.7 dB at BER ≈ 2×10^{-3} over the stated channel model. Moreover, the better BER performance of both the proposed MIMO schemes over multipath FSRF channel as compared to single-path FSRF channel is due to the use of the OFDM technique which helps mitigate the impact of the FSRF, providing more reliable wireless communication.

We have also compared the bit error performance of both the proposed MIMO schemes with that of the corresponding SA schemes over a multipath FSRF channel. The simulation results reveal that the STC-OFDM-MIMO and DSTC-OFDM-MIMO schemes clearly outperform the STC-OFDM-SA and DSTC-OFDM-SA schemes by a significant margin over multipath FSRF channel with BPSK modulation technique under both non-jamming and jamming environments for the entire SNR range under consideration. The BER curves show that the BER performance of STC-OFDM-SA and STC-OFDM-MIMO schemes both at the SNR of 3 dB without jamming is 6×10^{-2} and 8×10^{-5} respectively. Moreover, the BER performance of STC-OFDM-SA and STC-OFDM-MIMO schemes both at the SNR of 3 dB with jamming J/S = 23 dB is 7×10^{-2} and 2×10^{-4} respectively. It is also observed from the BER curves that the BER performance

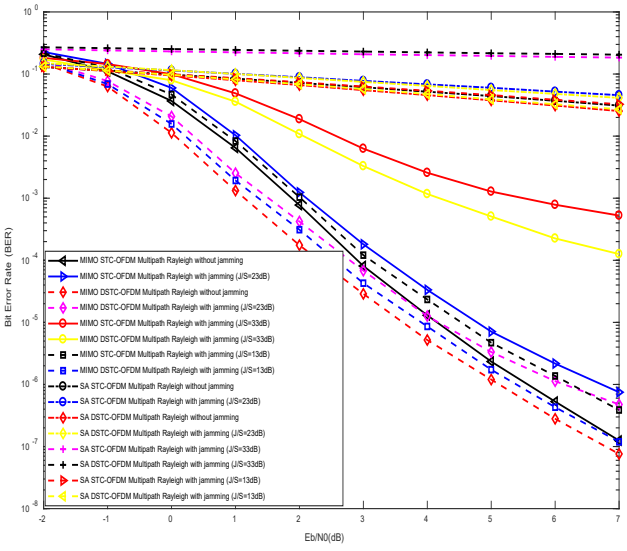

Fig. 8. The BER performances of the STC-OFDM-MIMO (Non-cooperative) scheme and the DSTC-OFDM-MIMO (Coded-cooperative) scheme over multipath FSRF channel with 9 taps, under different jamming scenarios with BPSK modulation technique, frame length l = 512, No. of frames = 100000 and 5 decoding iterations.

of DSTC-OFDM-SA and DSTC-OFDM-MIMO schemes both at the SNR of 3 dB without jamming is 5.5×10^{-2} and 3×10^{-5} respectively. Moreover, the BER performance of DSTC-OFDM-SA and DSTC-OFDM-MIMO schemes at the SNR of 3 dB with jamming J/S = 23 dB is 7×10^{-2} and 7×10^{-5} respectively. Furthermore, it is evident from the simulation results that the performance of the STC-OFDM-SA scheme with jamming J/S = 33 dB, is the worst among all the compared schemes over multipath FSRF channel.

6. Conclusion

In this research paper, an effective and innovative AJ technique based on the DSTC-OFDM scheme incorporated with Alamouti STBC-MIMO (2×2) antennas is proposed for a coded-cooperative wireless communication system under wideband noise jamming environment. The TCS is highly appropriate to be used in a typical cooperative communication framework. Therefore, the proposed scheme based on DTCs is effectively extended in coded-cooperative wireless communication system. As an appropriate benchmark for comparison and to validate the effectiveness of our proposed distributed scheme, a conventional STC-OFDM scheme with Alamouti STBC-MIMO (2×2) antennas has also been simulated and analyzed for non-cooperative wireless communication system under the same circumstances and noise jamming environment. Moreover, both the proposed MIMO schemes are compared with the corresponding SA schemes. In addition to BPSK modulation, both the proposed schemes have also been simulated and analyzed for higher-order modulation techniques, such as 4-QAM and 16-QAM. Soft-demodulators are employed along with the JISISO-MIMO (Turbo) decoding technique at the destination node for the proposed DSTC-OFDM scheme incorporating STBC-MIMO (2×2) antennas.

The Monte Carlo simulation results reveal that the DSTC-OFDM-MIMO scheme with Alamouti-STBC (2×2) antennas clearly outperforms the STC-OFDM-MIMO (non-cooperative) scheme by a gain that ranges between 0.5–6 dB for different jamming scenarios with J/S = 23 dB in the high SNR simulated region under the same conditions, i.e., the code rates R_c = 1/3 and data frame lengths l = 512 bits for both the proposed MIMO schemes. However, in the low SNR simulated region, the STC-OFDM-MIMO scheme shows similar performance as the DSTC-OFDM-MIMO scheme, under identical conditions. It is also evident from the Monte Carlo simulation results that the DSTC-OFDM-MIMO scheme achieves significant coding gain over the STC-OFDM-MIMO scheme over the slow FSRF channel as compared to the fast FSRF channel. Furthermore, the proposed distributed scheme with STBC-MIMO (2×2) antennas incorporates both cooperative diversity gain as well as coding gain. The bit error performance of the proposed DSTC-OFDM-MIMO scheme in coded-cooperation can further be enhanced by employing multiple relays. Moreover, massive MIMO antennas can be deployed at the destination node to further minimize the BER,

at the cost of increased hardware complexity and computational requirements.

Acknowledgments

The authors would like to express their gratitude to the editor and the reviewers for their valuable time, review comments, and suggestions that immensely contribute to improving the quality of this research paper.

References

[1] PIRAYESH, H., ZENG, H. Jamming attacks and anti-jamming strategies in wireless networks: A comprehensive survey. *IEEE Communications Surveys and Tutorials*, 2022, vol. 24, no. 2, p. 767–809. DOI: 10.1109/COMST.2022.3159185

[2] ZOU, Y., ZHU, J., WANG, X., et al. A survey on wireless security: Technical challenges, recent advances, and future trends. *Proceedings of the IEEE*, 2016, vol. 104, no. 9, p. 1727–1765. DOI: 10.1109/JPROC.2016.2558521

[3] ZHANG, L., RESTUCCIA, F., MELODIA, T., et al. Jam sessions: Analysis and experimental evaluation of advanced jamming attacks in MIMO networks. In *Proceedings of the International Symposium on Mobile Ad Hoc Networking and Computing (MobiHoc)*. 2019, p. 61–70. DOI: 10.1145/3323679.3326504

[4] JAGANNATH, A., JAGANNATH, J., DROZD, A. High rate-reliability beamformer design for 2×2 MIMO-OFDM system under hostile jamming. In *Proceedings of 2020 29th International Conference on Computer Communications and Networks (ICCCN)*. Honolulu (HI, USA), 2020, p. 1–9. DOI: 10.1109/ICCCN49398.2020.9209635

[5] LIANG, Y., REN, J., LI, T. Secure OFDM system design and capacity analysis under disguised jamming. *IEEE Transactions on Information Forensics and Security*, 2020, vol. 15, p. 738–752. DOI: 10.1109/TIFS.2019.2929449

[6] CHOI, H., PARK, S., LEE, H. N. Covert anti-jamming communication based on Gaussian coded modulation. *Applied Sciences (Switzerland)*, 2021, vol. 11, no. 9, p. 1–28. DOI: 10.3390/app11093759

[7] SKLAR, B. *Digital Communications: Fundamentals and Applications*. 2nd ed. Prentice Hall, 2017. ISBN: 978-0134724058

[8] MALEKI, M., MALIK, M., FOLKESSON, P., et al. Modeling and evaluating the effects of jamming attacks on connected automated road vehicles. In *Proceedings of 2022 IEEE 27th Pacific Rim International Symposium on Dependable Computing (PRDC)*. Bejing (China), 2022, p. 12–23. DOI: 10.1109/PRDC55274.2022.00016

[9] SIDEK, O., YAHYA, A. Reed-Solomon coding for frequency hopping spread spectrum in jamming environment. *American Journal of Applied Sciences*, 2008, vol. 5, no. 10, p. 1281–1284. DOI: 10.3844/ajassp.2008.1281.1284

[10] BALDI, M., BIANCHI, M., CHIARALUCE, F., et al. Advanced coding schemes against jamming in telecommand links. In *Proceedings of IEEE Military Communications Conference (MILCOM 2013)*. San Diego (CA, USA), 2013, p. 1220–1226. DOI: 10.1109/MILCOM.2013.208

[11] DAI, J., GUO, W., XU, D. The performance of LDPC coded frequency hopping system under follower jamming. In *2014 International Conference on Information and Communications Technologies (ICT 2014)*. Nanjing (China), 2014, p. 1–6. DOI: 10.1049/cp.2014.0613

[12] KAPLAN, A., CAN, M., ALTUNBAS, I., et al. Comparative performance evaluation of LDPC coded OFDM-IM under jamming attack. *IEEE Transactions on Vehicular Technology*, 2023, vol. 72, no. 5, p. 6209–6224. DOI: 10.1109/TVT.2022.3232491

[13] TAVAKKOLI, R. Performance evaluation of turbo code system under jamming environment. *Journal of Soft Computing and Decision Support Systems (JSCDSS)*, 2015, vol. 2, no. 3, p. 14–19. ISSN: 2289-8603

[14] PURWAR, A., JOSHI, D., CHAUBEY, V. K. GPS signal jamming and anti-jamming strategy. In *2016 IEEE Annual India Conference (INDICON)*. Bangalore (India), 2016, p. 1–6. DOI: 10.1109/INDICON.2016.7838933

[15] AHMED, E. S., HUSSEIN, A. A. Turbo code performance in the presence of jamming signals. In *The 11th Scientific Conference of the University of Babylon.* Baghdad (Iraq), 2009, p. 29–39. [Online]. Available at: https://www.researchgate.net/publication/215466329_Turbo_Code_Performance_in_the_Presence_of_Jamming_Signals

[16] BERROU, C., GLAVIEUX, A., THITIMAJSHIMA, P. Near Shannon limit error-correcting coding and encoding: Turbo-codes (1). In *IEEE International Conference on Communications.* Geneva (Switzerland), 1993, p. 1064–1070. DOI: 10.1109/icc.1993.397441

[17] MUGHAL, S., YANG, F., EJAZ, S., et al. Asymmetric turbo code for coded-cooperative wireless communication based on matched interleaver with channel estimation and multi-receive antennas at the destination. *Radioengineering*, 2017, vol. 26, no. 3, p. 878 to 889. DOI: 10.13164/re.2017.0878

[18] UMAR, R., YANG, F., XU, H. J., et al. Distributed turbo coded spatial modulation based on code matched interleaver for MIMO system. *Wireless Networks*, 2023, vol. 29, no. 5, p. 1995–2013. DOI: 10.1007/s11276-023-03256-1

[19] SENDONARIS, A., ERKIP, E., AAZHANG, B. User cooperation diversity. Part I. System description. *IEEE Transactions on Communications,* 2003, vol. 51, no. 11, p. 1927–1938. DOI: 10.1109/TCOMM.2003.818096

[20] SENDONARIS, A., ERKIP, E., AAZHANG, B. User cooperation diversity. Part II: Implementation aspects and performance analysis. *IEEE Transactions on Communications*, 2003, vol. 51, no. 11, p. 1939–1948. DOI: 10.1109/TCOMM.2003.819238

[21] LANEMAN, J. N., WORNELL, G. W., TSE, D. N. C. An efficient protocol for realizing cooperative diversity in wireless networks. In *IEEE International Symposium on Information Theory - Proceedings*. Washington (USA), 2001, p. 294–294. DOI: 10.1109/ISIT.2001.936157

[22] SOLIMAN, T., YANG, F., EJAZ, S., et al. Decode-and-forward polar coding scheme for receive diversity: A relay partially perfect retransmission for half-duplex wireless relay channels. *IET Communications.* 2017, vol. 11, no. 2, p. 185–191. DOI: 10.1049/iet-com.2016.0915

[23] SIMOENS, S., MUÑOZ-MEDINA, O., VIDAL, J., et al. Compress-and-forward cooperative mimo relaying with full channel state information. *IEEE Transactions on Signal Processing*, 2010, vol. 58, no. 2, p. 781–791. DOI: 10.1109/TSP.2009.2030622

[24] MESLEH, R. Y., HAAS, H., SINANOVIĆ, S., et al. Spatial modulation. *IEEE Transactions on Vehicular Technology*, 2008, vol. 57, no. 4, p. 2228–2241. DOI: 10.1109/TVT.2007.912136

[25] TASHATOV, N. N., SEKSEMBAYEVA, M. A., OVECHKIN, G. V., et al. Interference immunity and energy efficiency of digital communications systems in multipath channel with fading. *Indonesian Journal of Electrical Engineering and Computer Science*, 2022, vol. 27, no. 3, p. 1412–1418. DOI: 10.11591/ijeecs.v27.i3.pp1412-1418

[26] SU, W., SAFAR, Z., OLFAT, M., et al. Obtaining full-diversity space-frequency codes from space-time codes via mapping. *IEEE Transactions on Signal Processing*, 2003, vol. 51, no. 11, p. 2905 to 2916. DOI: 10.1109/TSP.2003.818200

[27] ALAMOUTI, S. M. A simple transmit diversity technique for wireless communications. *IEEE Journal on Selected Areas in Communications*, 1998, vol. 16, no. 8, p. 1451–1458. DOI: 10.1109/49.730453

[28] HUO, P., CAO, L. Distributed STBC with soft information relay based on Gaussian approximation. *IEEE Signal Processing Letters*, 2012, vol. 19, no. 10, p. 599–602. DOI: 10.1109/LSP.2012.2206383

[29] MHEIDAT, H., UYSAL, M., AL-DHAHIR, N. Distributed space-time block coded OFDM for relay-assisted transmission. In *IEEE International Conference on Communications*. Istanbul (Turkey), 2006, vol. 10, p. 4513–4519. DOI: 10.1109/ICC.2006.255350

[30] LIN, J. C. H., STEFANOV, A. Coded cooperation for OFDM systems. In *2005 International Conference on Wireless Networks, Communications and Mobile Computing*, 2005, p. 7–10. DOI: 10.1109/WIRLES.2005.1549376

[31] UMAR, R., YANG, F., MUGHAL, S. BER performance of a polar coded OFDM over different channel models. In *Proceedings of 2018 15th International Bhurban Conference on Applied Sciences and Technology (IBCAST).* Islamabad (Pakistan), 2018, p. 764–769. DOI: 10.1109/IBCAST.2018.8312308

[32] HUNTER, T. E., NOSRATINIA, A. Diversity through coded cooperation. *IEEE Transactions on Wireless Communications*, 2006, vol. 5, no. 2, p. 283–289. DOI: 10.1109/TWC.2006.1611050

[33] GAWANDE, P. D., LADHAKE, S. A. Optimal performance of convolution coded OFDM. In *Proceedings of the 2016 IEEE International Conference on Wireless Communications, Signal Processing and Networking (WiSPNET)*. Chennai (India), 2016, p. 335–338. DOI: 10.1109/WiSPNET.2016.7566150

[34] ELFITURI, M., HAMOUDA, W., GHRAYEB, A. A convolutional-based distributed coded cooperation scheme for relay channels. *IEEE Transactions on Vehicular Technology*, 2009, vol. 58, no. 2, p. 655–669. DOI: 10.1109/TVT.2008.927033

[35] TANG, L., YANG, F., ZHANG, S., et al. Joint iterative decoding for LDPC-coded multi-relay cooperation with receive multi-antenna in the destination. *IET Communications*, 2013, vol. 7, no. 1, p. 1–12. DOI: 10.1049/iet-com.2012.0038

[36] HU, J., DUMAN, T. M. Low-density parity-check codes over wireless relay channels. *IEEE Transactions on Wireless Communications*, 2007, vol. 6, no. 9, p. 3384–3394. DOI: 10.1109/TWC.2007.06083

[37] UMAR, R., YANG, F., MUGHAL, S. Turbo coded OFDM combined with MIMO antennas based on matched interleaver for coded-cooperative wireless communication. *Information,* 2017, vol. 8, no. 2, p. 1–16. DOI: 10.3390/info8020063

[38] SOLIMAN, T. H. M., YANG, F., EJAZ, S. Interleaving gains for receive diversity schemes of distributed turbo codes in wireless half-duplex relay channels. *Radioengineering*, 2015, vol. 24, no. 2, p. 481–488. DOI: 10.13164/re.2015.0481

[39] EJAZ, S., YANG, F. F. Jointly optimized Reed-Muller Codes for multi-level multi-relay coded-cooperative VANETS. *IEEE Transactions on Vehicular Technology*, 2016, vol. 66, no. 5, p. 4017–4028. DOI: 10.1109/TVT.2016.2604320

[40] UMAR, R., YANG, F. F., MUGHAL, S. Distributed Reed-Muller code with multiple relays for cooperative broadband wireless networks. *Radioelectronics and Communications Systems*, 2019, vol. 62, no. 9, p. 449–461. DOI: 10.3103/S0735272719090024

[41] MUGHAL, S., UMAR, R., YANG, F. F., et al. Distributed Reed-Muller coded-cooperative spatial modulation. *Wireless Personal Communications*, 2022, vol. 124, no. 3, p. 2785–2807. DOI: 10.1007/s11277-022-09489-1

[42] SOLIMAN, T., YANG, F., EJAZ, S. Decode and forward polar coding for half-duplex two-relay channels based on multilevel construction. *International Journal of Electronics*, 2016, vol. 104, no. 4, p. 539–554. DOI: 10.1080/00207217.2016.1218068

[43] UMAR, R., YANG, F., MUGHAL, S., et al. Distributed polar-coded OFDM based on Plotkin's construction for half duplex wireless communication. *International Journal of Electronics*, 2018, vol. 105, no. 7, p. 1097–1116. DOI: 10.1080/00207217.2018.1426118

[44] SOLIMAN, T., YANG, F. Cooperative punctured polar coding (CPPC) scheme based on Plotkin's construction. *Radioengineering*, 2016, vol. 25, no. 3, p. 482–489. DOI: 10.13164/re.2016.0482

[45] CHRONOPOULOS, S. K., CHRISTOFILAKIS, V., TATSIS, G., et al. Performance of turbo coded OFDM under the presence of various noise types. *Wireless Personal Communications*, 2016, vol. 87, no. 4, p. 1319–1336. DOI: 10.1007/s11277-015-3055-1

[46] UMAR, R., YANG, F. F., XU, H. J., et al. Distributed polar code based on Plotkin's construction with MIMO antennas in frequency selective Rayleigh fading channels. *Wireless Personal Communications*, 2019, vol. 104, no. 1, p. 287–306. DOI: 10.1007/s11277-018-6020-y

[47] VAN DER MEULEN, E. C. Three-terminal communication channels. *Advances in Applied Probability*, 1971, vol. 3, no. 1, p. 120–154. DOI: 10.2307/1426331

[48] BENEDETTO, S., DIVSALAR, D., MONTORSI, G., et al. A soft-input soft-output APP module for iterative decoding of concatenated codes. *IEEE Communications Letters*, 1997, vol. 1, no. 1, p. 22–24. DOI: 10.1109/4234.552145

[49] PICKHOLTZ, R. L., SCHILLING, D. L., MILSTEIN, L. B. Theory of spread-spectrum communications - A tutorial. *IEEE Transactions on Communications*, 1982, vol. 30, no. 5, p. 855 to 884. DOI: 10.1109/TCOM.1982.1095533

[50] SCHILLING, D. L., MILSTEIN, L. B., PICKHOLTZ, R. L., et al. Optimization of the processing gain of an M-ary DSSS communication system. *IEEE Transactions on Communications*, 1980, vol. 28, no. 8, p. 1389–1398. DOI: 10.1109/TCOM.1980.1094782

[51] THOMPSON, S. C., PROAKIS, J. G., ZEIDLER, J. R., et al. Constant envelope OFDM in multipath Rayleigh fading channels. In *Proceedings of the IEEE Military Communications Conference MILCOM*. Washington (USA), 2006, p. 1–7. DOI: 10.1109/MILCOM.2006.302187

[52] IEEE. IEEE STD 802.11A, *Supplement to IEEE Standard for Information Technology - Telecommunications and Information Exchange between Systems - Local and Metropolitan Area Networks - Specific Requirements Part 11: Wireless LAN Medium Access Control (MAC) and Physical Layer (PHY)*. IEEE, 1999, p. 1-102. DOI: 10.1109/IEEESTD.1999.90606

[53] DO, T. T., BJORNSON, E., LARSSON, E. G., et al. Jamming-resistant receivers for the massive MIMO uplink. *IEEE Transactions on Information Forensics and Security*, 2018, vol. 13, no. 1, p. 210–223. DOI: 10.1109/TIFS.2017.2746007

About the Authors ...

Agha M. Ali MIRZA (corresponding author) received his Bachelor of Engineering (B.E.) degree in Electrical Engineering from NED University of Engineering and Technology (NEDUET) Karachi, Pakistan, in 2002. He completed his M.Sc. degree in Radio and Mobile Communication Systems from the University of Hertfordshire, United Kingdom in 2009. Presently, he is working as a senior

lecturer in the Electrical Engineering Dept. of Sir Syed University of Engineering and Technology, Karachi, Pakistan. He is also currently pursuing his Ph.D. degree in Telecommunication Engineering from NEDUET Karachi, Pakistan. His research interests include channel coding, Turbo codes, OFDM, coded-cooperative communication, noise jamming and anti-jamming techniques.

Attaullah KHAWAJA received his B.E. degree in Electrical Engineering from Mehran University of Engineering and Technology, Pakistan in 1993, Master of Engineering (M.E.) degree in Electrical Engineering from NEDUET Karachi, Pakistan in 2002, and Ph.D. in Communication and Information Systems from Beijing Institute of Technology, P. R. China in 2007. Currently, he is working as a Professor and Chairman, in the Electrical Engineering Dept. of NEDUET Karachi, Pakistan. His academic career spans over 25 years and he has published several research papers in international journals and conferences in the fields of communications, robotics and image processing.

Shoaib MUGHAL received his B.S. degree in Electronic Engineering from Sir Syed University of Engineering and Technology (SSUET) Karachi, Pakistan, in 2008. In 2011, he obtained his M.E. degree in Telecommunication Engineering from NEDUET Karachi, Pakistan. He worked as a lecturer in the Electronic Engineering Dept. of SSUET Karachi, Pakistan, for three years. He completed his Ph.D. from the College of Electronic and Information Engineering, Nanjing University of Aeronautics and Astronautics, China in 2017. Presently, he is working as Head-of-Department, in the Computer Engineering Dept. of Bahria University Karachi Campus, Pakistan. His major research interests are MIMO systems, channel coding, and coded-cooperative diversity. He has authored several journal and conference papers.

Rizwan Aslam BUTT received his B.E. degree in Electronic Engineering, M.S. degree in CS/IT, and M.E. degree in Telecommunication Engineering from NEDUET Karachi, Pakistan in 2006, 2011, and 2013 respectively. He received his Ph.D. in Electrical Engineering from University Technology Malaysia in 2017. Currently, he is serving as an assistant professor in the Telecommunications Engineering Dept. of NEDUET Karachi, Pakistan from 2010 to till date. His research interests include optical communication networks, smart grid, nanogrid clustering and IOT. He has authored more than 80 journal and conference papers.